Reviewed Preprint
v1 • September 1, 2023
Not revised

Reviewed Preprint
v2 • March 20, 2026
Revised by authors

Systematic Analysis of Network-driven Adaptive Resistance to CDK4/6 and Estrogen Receptor Inhibition using Meta-Dynamic Network Modelling

Anthony Hart[1,2,3,4], **Sung-Young Shin**[1,2,3], **Lan K Nguyen**[1,2,3,4]

[1]Department of Biochemistry and Molecular Biology, Faculty of Medicine, Nursing and Health Sciences, Monash University, Clayton, Australia • [2]Biomedicine Discovery Institute, Monash University, Clayton, Australia • [3]Computational Systems Oncology Program, South Australian immunoGENomics Cancer Institute (SAiGENCI), The University of Adelaide, Adelaide, Australia • [4]Australian Research Council Centre of Excellence for the Mathematical Analysis of Cellular Systems (MACSYS), Canberra, Australia

For correspondence: lan.nguyen@adelaide.edu.au

Competing interests: No competing interests declared

Reviewing editor: Mariana Gómez-Schiavon, Universidad Nacional Autónoma de México, Mexico

eLife Assessment

This manuscript presents a **useful** computational framework for systematically characterising how heterogeneity in initial conditions or biophysical parameters shapes the dynamic behaviour of protein signalling networks, with potential relevance to understanding adaptive drug resistance. While the approach represents a significant methodological contribution, the extent to which its conclusions are biologically informative remains debated, as the model is only qualitatively compared with experimental data and lacks quantitative validation. As a result, the strength of evidence supporting the mechanistic claims is viewed as **incomplete**.

https://doi.org/10.7554/eLife.87710.2.sa2

Abstract

Drug resistance inevitably emerges during the treatment of cancer by targeted therapy. Adaptive resistance is a major form of drug resistance, wherein the rewiring of protein signalling networks in response to drug perturbation allows drug-targeted protein activity to recover. This can occur in the continuous presence of the drug and enables cells to survive/grow. Simultaneously, molecular heterogeneity enables the selection of drug-resistant cancer clones that can survive an initial drug insult, proliferate, and eventually cause disease relapse. Despite their importance, the link between heterogeneity and adaptive resistance, specifically how heterogeneity influences protein signalling dynamics to drive adaptive resistance, remains poorly understood. Here, we have explored the relationship between heterogeneity, protein signalling dynamics and adaptive resistance through the development of a novel modelling technique coined Meta Dynamic Network (MDN) modelling. We use MDN modelling to characterise how heterogeneity influences the drug-response signalling dynamics of the proteins that regulate early cell cycle progression and demonstrate that heterogeneity can robustly facilitate adaptive resistance associated dynamics for key cell cycle regulators. We determined the influence of heterogeneity at the level of both reaction coefficients and protein abundance and show that reaction coefficients are a much stronger driver of adaptive resistance. Owing to the mechanistic nature of the underpinning ODE framework, we then identified a full spectrum of subnetworks capable of driving adaptive resistance dynamics in the key early cell cycle regulators. Finally, we show that single-cell dynamic data supports the validity of our MDN modelling technique and a comparison between our

predicted resistance mechanisms and known CDK4/6 and Estrogen Receptor inhibitor resistance mechanisms suggests MDN can be deployed to robustly predict network-level resistance mechanisms for novel drugs and additional protein signalling networks.

Introduction

Drug resistance is a widespread phenomenon across all cancer types and is a major obstacle to the development of curative therapeutic strategies (1–3). Cellular heterogeneity is a known driver of drug resistance, wherein the treatment of a heterogenous population of cancer cells with cytostatic or cytotoxic drugs creates a selective pressure that results in the survival and expansion of any cells that are capable of overcoming the effects of said drugs (4–6). While this general phenomenon is well established (7–9), it is usually less clear exactly how and why some cells are able to overcome a drug treatment and others are not. Heterogeneity is a catch-all term used to describe any and all differences between cells, however, it could be argued that the majority of the differences between cells ultimately converge on differences in how their constituent proteins behave, i.e. their protein dynamics. To deepen our understanding of how tumour heterogeneity drives drug resistance, we must explore the relationship between cellular heterogeneity, protein dynamics and drug resistance.

The efficacy of a targeted therapy largely comes down to how well and how long the targeted protein is suppressed, and how frequently and reliably this suppression results in either cytostasis or apoptosis. A cell can therefore be considered resistant if the target protein is insufficiently suppressed or is initially suppressed but later recovers, or if the suppression of the protein is insufficient to stimulate cytostasis or apoptosis (10, 11). Proteins are embedded in complex networks and protein dynamics are dictated by the properties of the networks in which they reside. While resistance is often due to direct effects, such as reduced drug-target binding affinity (12, 13) or excessive drug efflux from tumour cells (14, 15), it can also occur due to changes in the state of the biochemical networks of a cell that counteract the effects of the drug; a phenomenon referred to as adaptive resistance (16–18). PI3K, EGFR and CDK4/6 are just few prime examples of proteins that have been targeted in the treatment of cancer that display acute and robust adaptive resistance (19–21). These studies also support the notion that it is rarely the behaviour of a single 'gatekeeper' protein that drives adaptive resistance, but an entire protein network that acts and is acted upon by the target protein (22, 23). Frequently however, we possess a limited knowledge and appreciation of the network-level mechanistic relationships that underpin adaptative resistance.

Understanding the relationship between cellular heterogeneity and adaptive drug resistance requires an ability to explore and characterise the heterogeneity that exists both within a tumour and between patients. This can be achieved *in silico* by investigating the behaviour of a network, i.e. the dynamics of its constituent proteins, over a broad range of network conditions, allowing us to observe the full spectrum of possible dynamics that can be displayed by a given network topology. A particularly useful technique for investigating protein signalling networks is Ordinary Differential Equation (ODE) modelling (24). An ODE model is a mathematical representation of how the protein species within a network interact and evolve over time. ODE models have been extensively used to simulate and predict network-level responses to perturbations, such as growth-factor stimulation or drug treatment (25–28). In an ODE model, the interactions between the network's constituent proteins are converted into mathematical formulations using well-established biochemical rate laws (29–33). The end result is a set of ODEs – the model – that can be numerically solved using specialised ODE solvers, allowing one to simulate, and thus predict, how the concentrations of the protein species will change over time or in response to perturbations (29–33).

An ODE model is comprised of state variables, initial conditions, model parameters, and defined inputs and outputs (29–31). Typically, the parameters, or reaction coefficients, represent the strength of protein interactions and state variables correspond to the concentrations of the protein species. Initial conditions (ICs) are the values of the state variables at the starting point of a simulation and represent the total abundance levels of the protein species within the model. Model input(s) are usually a perturbation to the modelled network, such as a growth factor

stimulation or a drug inhibition. We can model network heterogeneity by producing a suite of ODE models, each with their own set of parameter values and/or initial conditions. In this manner, each model 'instance' represents a unique cellular context and produces a unique set of dynamic behaviours for its constituent proteins. By varying the parameters and initial conditions over wide ranges, we can delineate an extreme upper limit to the heterogeneity in dynamics facilitated by a network topology.

The process of creating models almost always involves a degree of abstraction, either explicitly, due to conscious decisions by the creator, or implicitly, due to imperfect knowledge of the system being modelled. This abstraction forces a model's parameters to capture information beyond that which is being explicitly modelled and can potentially render the concept of a 'true' or 'biologically accurate' parameter value less meaningful. There is an array of factors that can influence reaction coefficients: post-translational modifications, catalysts/scaffolds, pH, etc., and they can all individually influence reaction coefficients over several orders of magnitude. In the context of cancer, this variability in reaction coefficients can become extreme, with mutations altering the properties of proteins and dramatically changing how strongly they interact with other proteins. By varying the parameters and initial conditions over wide ranges, we also potentially capture protein dynamics driven by factors we haven't explicitly modelled.

Drug resistance is a problem almost as old as drug treatments; and many computational modelling frameworks have been developed to investigate the emergence of drug resistance during cancer treatment (34–36). A comprehensive review of the modelling frameworks developed to explore the relationship between cellular heterogeneity and drug resistance, in particular, was written by Chisholm et al. in 2016 (35). Most of the models covered within focused on population dynamics and were used to identify key processes that govern how resistance emerges within a heterogenous cell population. Notably, none of the models in this review attempted to link heterogenous intracellular processes with adaptive resistance mechanisms, or resistance in general. Perhaps most similar to the ensemble approach developed within this project, He et al. developed an ODE-based modelling technique termed RACIPE (random circuit perturbation) (37). In contrast to our work, RACIPE was a quasi-Monte Carlo method developed to alleviate the necessity of identifying precise kinetic parameter values on which model predictions are supposedly dependent. While their technique does involve the exploration of a range of parameter values, it does so to make predictions about broadly robust outcomes in gene regulatory circuits, not to link parameter variation to heterogenous protein network dynamics. Thus, there is a need for a novel computational framework capable of systematically characterising network-dynamic heterogeneity and its relationship with adaptive resistance.

To address this need, we have developed a new modelling framework, coined Meta-Dynamic Network (MDN) modelling, which enables us to study the effects of network heterogeneity on protein signalling dynamics. In this paper we have applied MDN modelling to an Early Cell Cycle (ECC) network model to systematically explore and illuminate adaptive resistance mechanisms that arise in response to targeted CDK4/6 and Estrogen Receptor (ER) inhibition. The ECC network model developed herein incorporates the two major mitogenic signalling pathways that are largely responsible for cell cycle initiation, and the G1-S phase cell cycle regulatory network.

Using MDN and the ECC network model, we have demonstrated that variation in both the strength of reaction coefficients (parameters) and the total abundance of proteins (initial condition values) can affect the qualitative shape and features of a network's protein dynamics. Furthermore, we provide evidence that parameter variation induces a much greater variety in the qualitative shape and features of the network's protein dynamics and is therefore much more likely to give rise to adaptive resistance dynamics. We also show that there is a surprising large number of contexts in which the network topology of the ECC network can facilitate resistance dynamics, and that we can dissect these contexts to systematically characterise their underpinning kinetic drivers. Finally, we analysed existing publicly available biological data to qualitatively validate the existence of a spectrum of signalling dynamics in response to CDK4/6 inhibitors and propose a novel relationship between population signalling dynamics and population level drug sensitivity.

Materials and methods

ODE model construction, modelling, and simulations

We converted the ECC network (Figure 1) into a system of ODEs using standard biochemical rate laws: catalysed reactions (e.g. phosphorylations) as pseudo-first-order, complex formations as mass action, and transcription, translation and degradation as first-order kinetics. We used these simpler forms to reduce the number of poorly constrained parameters and enable a broader sampling of parameter values in the meta-dynamic analysis. The model comprises 50 state variables, 94 parameters, two mitogenic inputs and two drug inputs. A detailed description of model scope and justification is given in the Supplementary Information; and the biochemical reaction lists, ODEs and SBML model files are provided as Model Files S1 - S3.

Simulations were implemented in MATLAB (The MathWorks. Inc. 2019a) with IQM toolbox (*http://www.intiquan.com/intiquan-tools/*) to auto-generate ODEs and compile a MEX file for accelerated simulation speed. ODEs were solved using the SUNDIALS CVODES solver, which employs a variable-order, variable-step Backward Differentiation Formula (BDF) method, designed to solve stiff ODE systems.

Each simulation of our model consisted of three phases: (i) **starvation** phase to ensure a steady state equilibrium was reached before mitogenic stimulation; (ii) **fed** with constant mitogenic stimulation (100 nM of insulin and FGF) until quasi-steady state; and (iii) treatment with CDK4/6i and ER inhibitor. Mitogens and drugs were modelled as step inputs at the start of their respective phases and then held constant for the remaining simulation time, isolating network-intrinsic adaptation rather than responses to input removal. Drug inhibitions were modelled by reducing the relevant parameter values by a fixed fraction.

Sampling and filtering of model instances

MDN modelling involves random sampling of parameter sets to create unique model instances. We drew random parameter sets and conserved-total initial conditions and continued sampling until we obtained N=100,000 accepted instances for each analysis. To ensure sampled parameter sets reflected plausible biological contexts while retaining rare network states, we applied several filtering steps. An instance was accepted if it met the following: (i) **Quasi–steady state** reached in the starvation and fed phases, defined by very small changes across species within a time cap (1% change in concentration over the final 100 time steps); (ii) **Non-trivial on-target drug effect** during treatment (e.g. ≥5% reduction in the CDK4/6 activity proxy or [CDK4/6·CycD] level for CDK4/6i, and in [active ER] level for ERi). Moreover, we note that multi-timescale signalling models are often stiff (38, 39), and random parameter draws can create extreme early transients that are numerically hard to integrate even with stiff solvers. We therefore excluded these parameter instances, which accounts for only <1% of total sampled sets.

Applying these filters, ~40–45% of instances did not reach steady state within the allotted time, and ~50–55% did not meet the minimum drug-response criterion. Approximately 10% satisfied all criteria and were retained for analysis. Importantly, we employed 'rejection sampling' and continued drawing until we had N = 100,000 accepted instances that satisfied all the criteria.

Quantitative definitions of dynamic patterns

A major component of MDN modelling is the analysis of the qualitative shape of individual protein dynamics. This enables us to group together model instances that produce broadly similar behaviours for any proteins being investigated. We can then analyse these groups to identify and elucidate shared network structures that drive the behaviour. To this end, we defined six qualitative protein dynamic categories: increasing, decreasing, biphasic, rebound, no-response and other.

To assess the qualitative shape of each protein dynamic, we developed a series of mathematical restraints that were capable of sorting protein simulations into their appropriate categories.

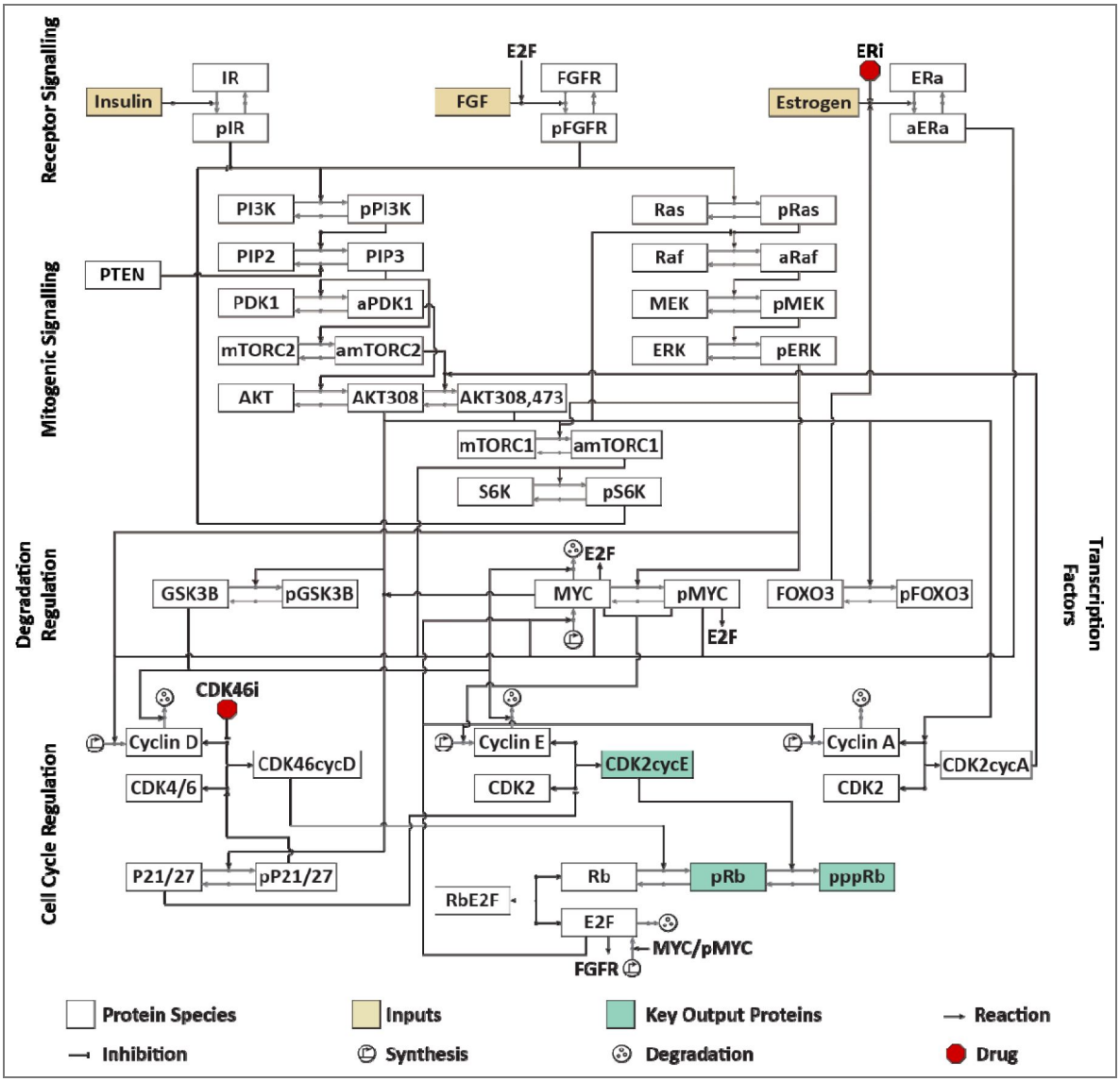

Figure 1. Network Schematic of the Early Cell Cycle (ECC) Network.

Network schematic showing the detailed biochemical reactions that regulate the initiation of the G1 phase and transition through to the S phase of the cell cycle. The network includes three mitogenic inputs, two mitogenic signalling pathways, PI3K and MAPK, key transcription factors that promote G1 phase transition, key CDK-cyclin complexes and their regulators, a CDK4/6 inhibitor, and an estrogen receptor inhibitor. Canonically, mitogenic stimulation leads to the cascading activation of the mitogenic signalling pathways, which converge on the synthesis of cyclin D. The synthesis of cyclin D then promotes the activation of CDK4/6, which consequently drives the synthesis of cyclin E. Cylin E activates CDK2, leading to the synthesis of cyclin A and the formation of CDK2-cyclin A complexes signals the initiation of S phase. ER and CDK4/6 inhibitors are believed to disrupt this linear chain of events and thus prevent proliferation.

First, each protein dynamic was normalised to its initial value. A protein's dynamic was categorised as **increasing (INC)** if (*i*) the final concentration exceeded 20% of its initial concentration, (*ii*) over the entire simulated time period it never dropped below 10% of its initial concentration, and (*iii*) the final concentration was within 10% of the maximum concentration. It was categorised as **decreasing (DEC)** if (*i*) the final concentration was at least 20% lower than the initial concentration, (*ii*) never went above 10% of its initial concentration, and (*iii*) the final concentration was within 10% of the minimum concentration. It was categorised as **biphasic (BIP)** if (*i*) the maximum concentration exceeded the initial concentration by 20% and (*ii*) the final concentration was at least 10% lower than the maximum concentration. It was categorised as **rebound (REB)** if (*i*) the minimum concentration was at least 20% lower than the initial concentration and (*ii*) the final concentration was at least 10% bigger than the minimum concentration. It was categorised as **no-response (NRP)** if the concentration never exceeded more or less than 10% of the initial concentration. Finally, it was categorised as **other (ETC)** if the protein's dynamic did not fit one of the previously described categories.

Key model output proteins

There is strong evidence to suggest that the linear cascade of cell cycle regulator progression, wherein the activation of CDK4/6 leads to the activation of CDK2-cyclin E complex, which in turn leads to the activation of CDK2-cyclin A, is overly simplistic (40, 41). If this traditional understanding was correct, the inhibition of CDK4/6 activity would robustly inhibit cell cycle progression, yet this is not the case (42). A number of studies have suggested that the activation or reactivation of proteins downstream of CDK4/6 can enable a cell to overcome the cell cycle inhibitory effects of CDK4/6 targeting drugs and enable cell cycle progression. Proteins that have been shown to demonstrate this phenomenon include phosphorylated Rb and the active CDK2-cyclin E complex (21, 43, 44). As such, we have focused on the dynamics of monophosphorylated Rb (**pRb**), hyperphosphorylated Rb (**pppRb**) and the CDK2-cyclin E complex (**CDK2cycE**) throughout this project, as key mediators of adaptive resistance to CDK4/6 and ER inhibitors.

Protein knockdown perturbation analyses

To assess the effects of parameters on protein dynamics we performed high-throughput perturbation analyses wherein each parameter was knocked down one at a time (OAT) and the effect on the nominated output assessed. We chose the OAT design intentionally to obtain causal, first-order attribution of control points across a broad parameter ensemble without confounding from simultaneous co-inhibition. This provides an interpretable ranking of primary drivers that is consistent with the paper's mechanistic focus.

Results

An Overview of Meta-Dynamic Network (MDN) Modelling

To explore the link between cellular heterogeneity, protein dynamics and drug resistance, we first developed a novel modelling framework coined Meta-Dynamic Network (MDN) modelling. The principal purpose of the MDN modelling framework is to explore how parametric and initial condition variation influence the qualitative shape of protein dynamics within a given network. By varying model parameters and initial condition (**IC**) values we are able capture many sources of cellular heterogeneity and characterise their influence on protein signalling dynamics. Varying parameter values captures heterogeneity in the interactions between proteins that arises due to phenomena such as cell-specific mutations, post-translational modifications, and epigenetic modifications. Varying initial condition values captures heterogeneity in protein concentration that arises due to phenomena such as stochastic protein expression, copy number variation and tissue-specific expression programmes.

Once a large number of unique model instances have been generated, each with their own unique parameter and/or initial condition values, we can simulate each model's response to drug treatment and analyse the resulting shape of each protein's dynamic. From this analysis we can

determine if there are contexts where key output proteins, such as downstream targets of the drug perturbation, demonstrate protein dynamics associated with adaptive resistance. Finally, we can group model instances that display similar dynamics together and perform further analyses to systematically identify the mechanistic causes capable of driving adaptive resistance dynamics. An overview of the MDN modelling process can be seen in Figure 2.

Protein dynamics that are associated with adaptive resistance are those where the protein is insufficiently suppressed over a sustained time period, i.e. increasing, biphasic and rebound (18–20, 22, 45). Increasing is the most dramatic adaptive-resistance response, where the drug perturbation not only fails to suppress key output proteins, but actually increases their activity/expression. Biphasic is similar to increasing in its initial phase, where the outputs actually increase, however the degree of the second decreasing phase likely influences the degree of resistance conferred by this particular behaviour. Rebound is similar to biphasic wherein the degree of resistance conferred by this dynamic is likely influenced by how strongly the protein recovers. While rebound is probably the most commonly observed adaptive-resistance driving dynamic (18–23), for the purpose of this project we consider all three of these behaviours as adaptive-resistance associated behaviours and consider decreasing as the only sensitivity associated behaviour.

Construction of a mechanistic model of the Early Cell Cycle (ECC) network

The ECC network model generated in this project was built to capture the signalling events driving entry into G1 and progression through the early cell cycle events, up to the G1-S phase transition. A detailed network schematic of the ECC's biochemical reactions can be seen in Figure 1. We nominally include two Tyrosine Kinase Receptors (TKRs), the Insulin Receptor (INSR) and the Fibroblast Growth Factor Receptor (FGFR), as they strongly stimulate the PI3K and MAPK pathways respectively but are both capable of stimulating each pathway.

The two major mitogenic signalling pathways, PI3K and MAPK, were included for three reasons. The first is that they are known to potently stimulate the production of cyclin D, the primary activator of CDK4/6 (46, 47). The second is that activating mutations in these pathways are some of the most common mutations across all cancer types and the final reason is that these same mutations have been shown to facilitate resistance to CDK4/6 inhibitors (48, 49). The inclusion of proteins within this network is not exhaustive, due to computational limitations, but our model captures the core signalling relationships and network structure. The final component included in this model was the network regulating G1 entry and progression into S phase. This includes the relevant CDKs, cyclins and their inhibitors, as well as the transcription machinery regulating cyclin expression. Clinical approval for the use of CDK4/6 inhibitors has traditionally been limited to patients with ER+ (estrogen receptor-positive) breast cancer who were concurrently receiving ER (estrogen receptor) antagonists but were still experiencing disease progression (50–52). Due to the ER's ability to promote CDK4/6 inhibition efficacy and the clinical practice of simultaneously prescribing ER antagonists with CDK4/6 inhibitors (50–52), the ER and its downstream signalling events were also included in the model.

The ECC network model was constructed using ODEs that represent biochemical interactions as a series of ordinary differential equations based on established kinetic laws. More detailed description of the model is given in the **Methods and Materials**. The full ODE equations and reaction rates are given in supplementary Model Files S1 - S3.

The ECC network robustly facilitates resistance-associated protein dynamics

To investigate the meta-dynamics of the ECC network, i.e. the range of dynamics that can be facilitated by the topology of the ECC network, we first generated 100,000 unique model instances. Each model instance possessed an identical set of ICs along with a unique set of parameter values. The parameter values for each model instance were generated by randomly selecting values for

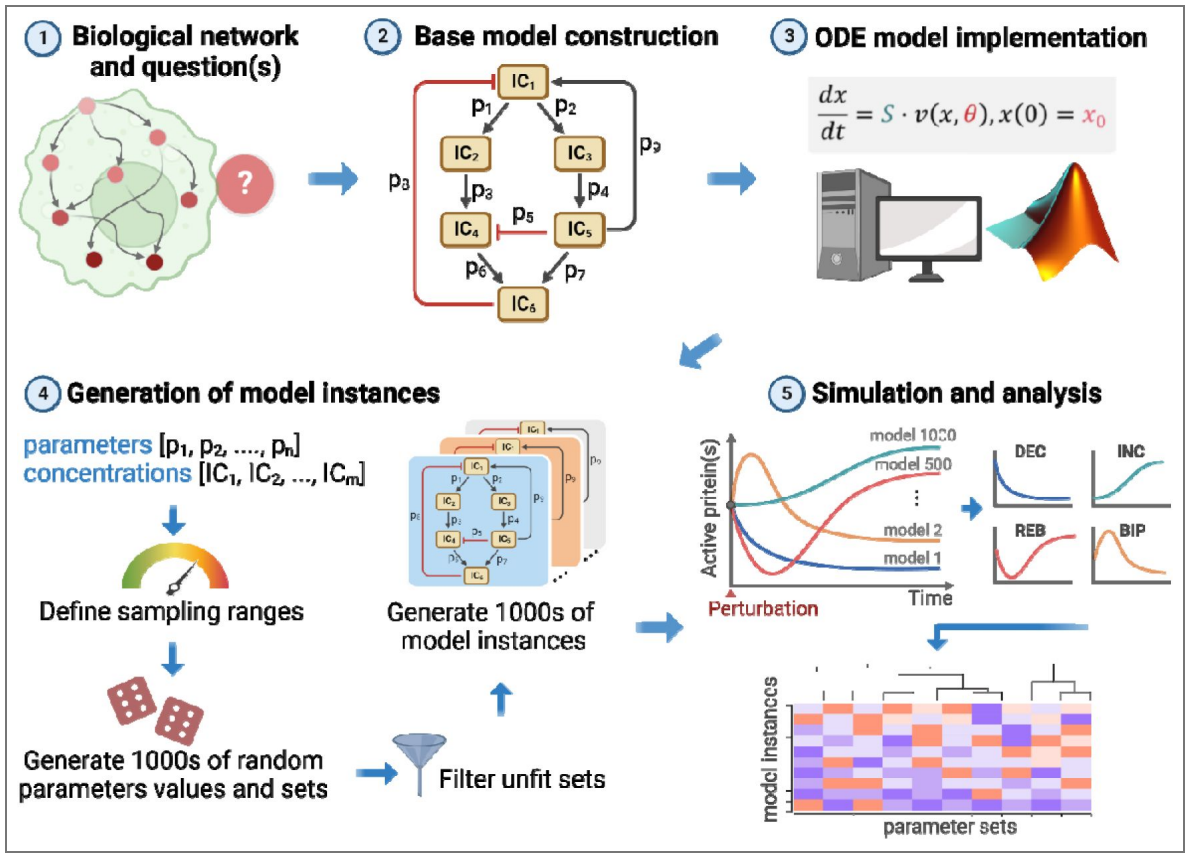

Figure 2. A workflow of the Meta Dynamic Network (MDN) modelling pipeline.

As with all modelling, the first step is asking a useful question. In our case this is usually related to understanding complex protein signalling dynamics. The second step is defining the network; this involves selecting nodes and identifying relationships between them. The third step is translating the network schematic to a mathematical representation, which is typically a combination of ordinary differential equations and biochemical rate laws. The fourth step is the generation of thousands of model instances, each with a unique set of properties e.g. parameter and initial condition values. The fifth step is the simulation of each model instance and the bulk analysis of the simulations. In this work, we analyse the distribution of the qualitative dynamics of the network's protein species.

each parameter between the range 10^{-5} to 10^{4}. See supplementary Figure S1A for a visual representation of the model generation process. Each model instance was simulated as laid out in the *ODE model construction, modelling, and simulations* (see **Methods and Materials**), and the resulting time-course drug response of each of the network's proteins was stored. This was repeated for all model instances. Alongside this process we also performed an experiment to test if novel, randomly drawn sets of model instances produced altered distributions of dynamics. Selecting new sets of 100,000 model instances produced near identical distributions of dynamics giving us confidence the distribution of protein dynamics converges at this set size. Details of this experiment can be found in the Supplementary Information.

We found that parameter variation resulted in a wide range of drug perturbation responses for many of the ECC network proteins. For example, Figure 3A displays a clustered subset of monophosphorylated Rb (pRb) time-course drug responses, showing a fairly extreme variety of drug-response dynamics that are possible in response to parameter variation. pRb not only possesses a *quantitative* spectrum of intra-category responses, which is probably expected, but it can also display a range of *qualitative* dynamics, and in fact, can demonstrate all six categories of qualitative drug response dynamics (see **Methods and Materials**).

Categorising the dynamics of each protein across all of the model instances allowed us to calculate the distribution/frequency of each dynamic for each protein. The distribution of behaviours for the 'active' forms of the model's protein species can be seen in the heatmap in Figure 3B. This overall distribution of protein behaviours is akin to a map that shows how the network state can affect the response of individual proteins to a drug treatment, in this case, the response to simultaneous CDK4/6 and ER inhibition. For many proteins, particularly proteins far upstream of the drug targets, the network state has only a little influence on drug response. This is particularly well demonstrated by the proteins in cluster 1, which show close to 100% no-response (NRP) dynamics.

Other proteins are much more strongly influenced by network state, where under the right conditions, a protein's response can flip from sensitivity to resistance. The proteins in clusters 4 and 5 show this phenomenon to a moderate degree but also show a predilection towards decreasing dynamics. The predilection to a decreasing dynamic may be due to their proximity to the drug targets CDK4/6 and ER and/or the linearity of the interactions between these proteins and the direct drug targets. It is particularly interesting to observe that most of the major promoters of cell cycle progression downstream of CDK4/6 cluster together (cluster 3, Figure 3B) and are all strongly influenced by the network state. This suggests that heterogeneity can strongly influence whether CDK4/6 inhibition will translate to an effective network-level response and prevent cell cycle progression.

To further assess the capability of the ECC network to facilitate adaptive resistance, we dug into the dynamic distributions of the key output proteins: pRb, pppRb (hyper-phosphorylated Rb) and CDK2cycE. Recall that we have defined resistance dynamics as increasing, biphasic and rebound, and sensitive behaviours as decreasing. While the frequency of sensitive dynamics was much higher than even the sum of resistance dynamics for all three proteins, the ratio of model instances displaying sensitivity to those displaying resistance was much lower than we expected. The ratios of sensitive to resistant behaviours, as percentages of 100,000 model instances, were 30:14, 22:8, 19:11 (rounded) for pRb, pppRb and CDK2cycE, respectively (see supplementary Figure S2A). These results suggest that for every 2 model instances/network states that facilitate sensitivity, there is 1 that facilitates resistance.

We then analysed the model instances further to identify how frequently sensitive and resistant behaviours occurred simultaneously across the three key output proteins. Our results suggest that broad sensitivity across all three output proteins is quite rare, and that resistance is remarkably common (Figure 3C). We observed that only 2.79% of model instances show simultaneous sensitivity across all three output proteins (Figure 3C). In contrast, when evaluating model instances where at least 1 of the output proteins displays a resistance associated dynamic, we observe that this occurs in just over a quarter, 26.04%, of all model instances (Figure 3C).

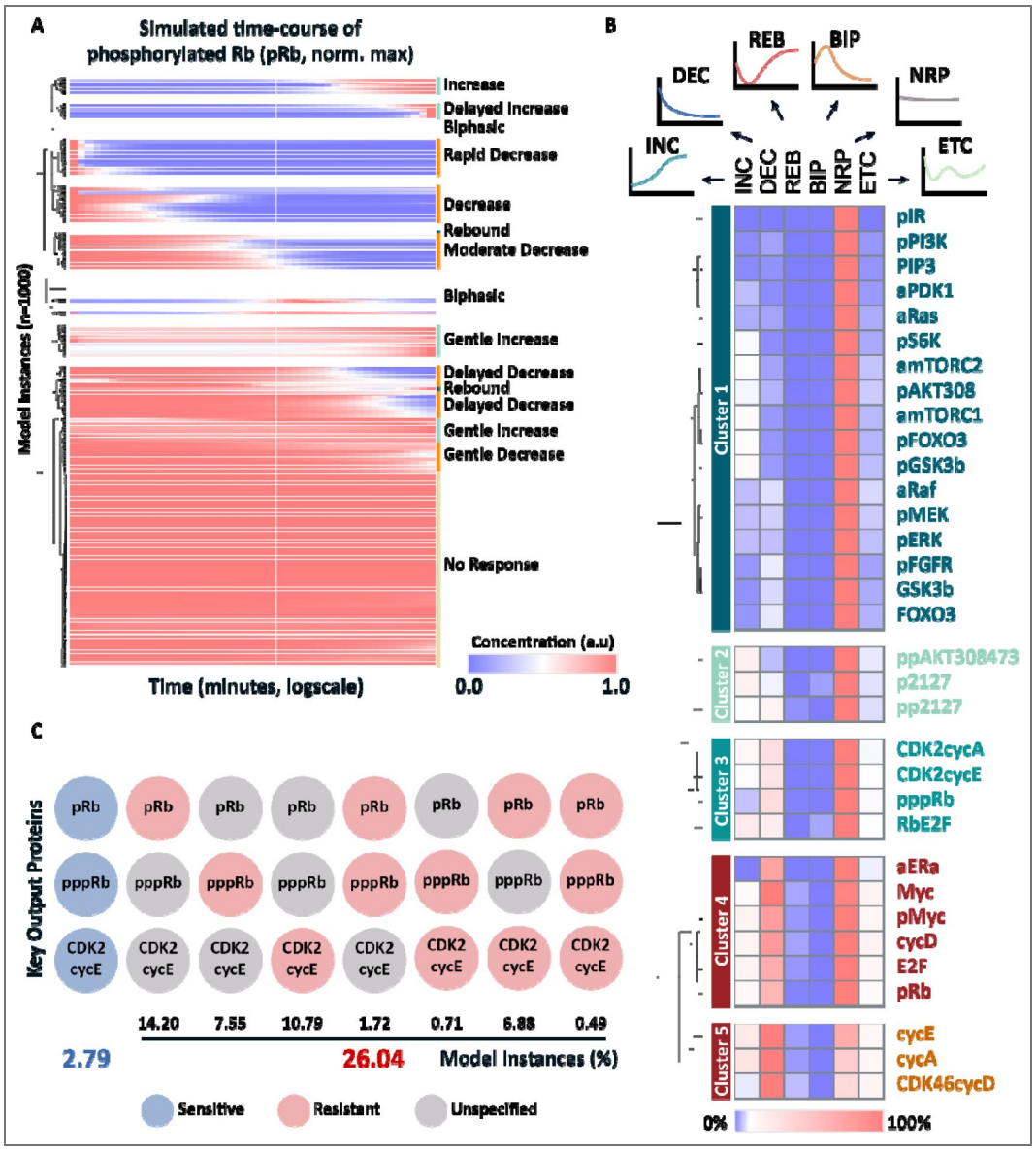

Figure 3. The ECC network robustly facilitates resistance-associated protein dynamics.

A) Clustered heatmap of a the time-course profiles of a representative subgroup model instances, normalised to maximum value. Time-course profiles are of mono-phosphorylated Rb (pRb), the downstream target of active CDK4/6, and in response to CDK4/6 and ER inhibition. Blue represents low concentration and red represents high concentration. **B)** The frequency of the 6 dynamic categories for the model's active protein forms, across 100,000 model instances. Blue represents low frequency and red represents high frequency. Species have been clustered to highlight species that have highly correlated distributions of dynamics. **C)** The frequency of model instances displaying simultaneous sensitivity (blue), or resistance in at least one of the key output proteins (red). Only 2.79% of model instances show simultaneous sensitivity across all three key output proteins. The percentage of resistant model instances was calculated by measuring the number of unique model instances that show resistance-associated dynamics for at least one of the key output proteins.

Given that CDK46cycD is only strongly suppressed in just under 60% of the model instances (supplementary Figure S2A), we hypothesised that the resistance displayed by the key output proteins may be largely due to insufficient suppression of CDK46cycD. To explore this, we filtered out the model instances that showed strong suppression of CDK46cycD and re-generated the distribution of protein dynamics. The resulting heatmap can be seen in supplementary Figure S2B. Surprisingly, the distribution of behaviours did not appear to change significantly, with the key output proteins showing very similar levels of adaptive resistance dynamics. This result suggests that the resistance dynamics of the key output proteins are *bona fide* adaptive resistance mechanisms and not just a result of insufficient suppression of the drug target.

Taken together, these results show that in the face of heterogeneity, the ECC network is robustly capable of facilitating adaptive resistance and that key output proteins display adaptive resistance even when the drug targets are being robustly suppressed.

Reaction coefficients are a stronger driver of adaptive-resistance dynamics than protein abundance

Having investigated the influence of parametric variation on drug response, we then wanted to explore the effect of IC variation in a similar fashion. To this end, we generated a further 100,000 model instances. This time, however, each model instance possessed an identical 'nominal' parameter set (see supplementary Table S1), along with a unique set of ICs. Each unique set of ICs was generated by randomly selecting values between the range 10^0 and 10^4, for the inactive form of each protein. See supplementary Figure S1B for a visual representation of the model generation process. We then repeated the simulation and analysis of protein dynamics as performed previously. The resulting distribution of dynamics can be seen in supplementary Figure S3A, and the clustering of this distribution can be seen in supplementary Figure S3B.

Interestingly, we found that compared to parametric variation, IC variation induced much less variety in protein response dynamics. Most proteins demonstrated a singular dominant behaviour and very few proteins exhibited both sensitive and resistance dynamics. This seems to suggest that IC variation is less capable of influencing a proteins drug response. However, we thought that this may have been due to the selected nominal parameter set and may not be a universal phenomenon. To explore this hypothesis, we investigated the ability of parametric variation and IC variation to induce adaptive resistance in our key output proteins. Essentially, we selected sensitive model instances, then randomly varied either parameter values or ICs and measured how frequently the model instance switched from drug-sensitive to drug-resistant.

To achieve this, we first selected 1000 unique parameter sets and 1000 unique sets of ICs that demonstrated a decreasing dynamic for one of our key output proteins, e.g. pppRb. Each parameter set was combined with each IC set, resulting in the creation of 1,000,000 unique model instances. These model instances were arranged in a 1000 x 1000 matrix, where the rows represent the unique parameter sets and the columns represent the unique ICs. See supplementary Figure 1C for a visual representation. Each model instance was simulated, and the dynamic of the key output protein recorded in the matrix. By measuring the frequency of resistant dynamics across the rows and columns, we could compare the ability of parameter variation and IC variation to induce resistance. An overview of this process can be seen in Figure 4A.

We found that for most parameter sets, varying the initial conditions *never* induced resistance in any of the three output proteins (Figure 4B, left). There was however, a very small number of parameter sets where altering the initial conditions frequently induced resistance. In contrast, altering the parameter values *always* induced resistance in a small number of the IC sets; but there were no IC sets wherein parameter variation strongly induced resistance, independent of the protein chosen (Figure 4B, right).

To further characterise the difference between parameter and IC variation, we then investigated the variety of dynamics induced by either parameter or IC variation. For each master parameter or IC set, we measured how many unique dynamic categories were produced across their

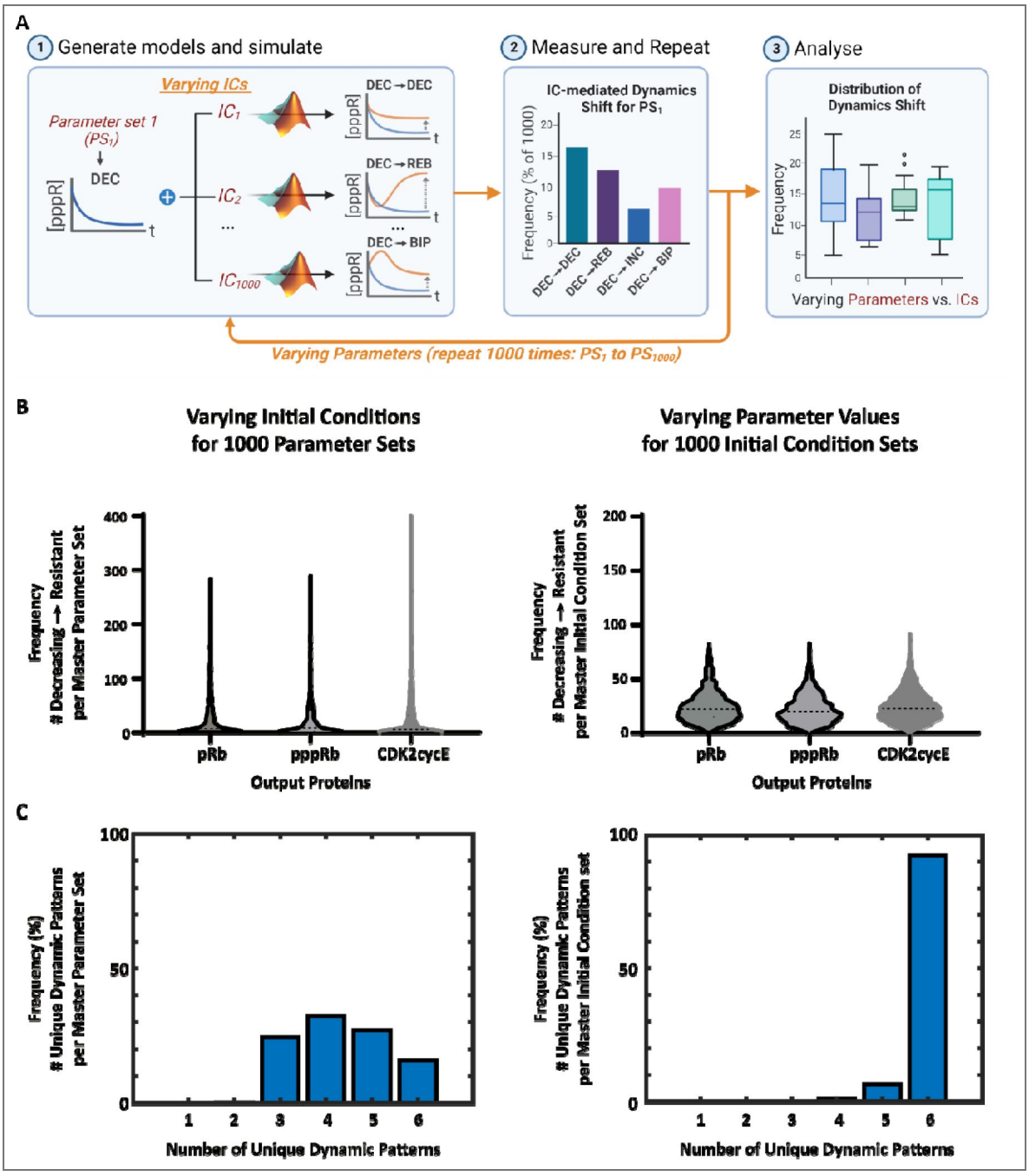

Figure 4. Reaction coefficients are a stronger driver of adaptive-resistance dynamics than protein abundance.

A) Overview of the computational pipeline undertaken to compare the effects of parametric variation with initial condition variation. 1000 unique initial condition sets are applied to a base parameter set that demonstrates a decreasing dynamic for the key output protein being analysed. Each of the new model instances are simulated and the category of the output protein's dynamic is determined. Then the number of times the model instances produce a resistance-associated dynamic is measured. This entire process is repeated for 1000 base parameter sets. The final step is measuring the distribution of resistance behaviours when the parameter values are changed and comparing the distribution when the initial condition values are changed. **B)** The frequency of which initial condition variation (left) induces resistance, in each key output protein. Varying initial condition values usually does not induce resistance, however, for select parameter sets, most initial conditions produce resistance associated dynamics. This analysis is repeated for parameter variation (right). Contrary to varying initial condition values, varying parameters usually induces resistance to a small degree, but there are no sets of initial conditions that are universally resistant. **C)** The number of unique dynamic categories produced by initial condition variation (left), versus parametric variation (right). Varying initial conditions produces a moderate variety of qualitative dynamics, and can produce all 6 dynamic categories, but varying parameters almost always induces every single possible dynamic category for the key output proteins.

respective 1000 model instances. We found that varying the ICs still induced a moderate amount of variety in protein dynamics (Figure 4C, left). However, parameter variation almost always produced all six dynamic categories (Figure 4C, right).

These results provide clear evidence that changes in both parameter values and initial condition values can facilitate the emergence of adaptive resistance. Because conserved totals shift the steady-state values even with fixed kinetics, expression heterogeneity (via totals) can alter pre-treatment equilibria and subsequent drug responses. Supplementary Figure S4 demonstrates this shift. However, changes in parameter values appear to be much more capable of inducing large, qualitative shifts in protein dynamics compared to changes in initial condition values.

The ability of expression variation to induce resistance also seems to be dependent on the master parameter set and there also appears to be no IC set that can induce resistance independent of the parameter values. These results imply that heterogeneity in reaction coefficients is much more likely, and independently able to facilitate the emergence of adaptive resistance compared to heterogeneity in protein abundance. Due to the *independent* ability of parameter variation to *strongly* induce adaptive resistance, we chose to focus on this particular form of heterogeneity in the following studies.

Reaction coefficients co-ordinate to drive adaptive resistance, independent of their individual strengths

The data produced by our initial MDN pipeline enabled us to identify thousands of model instances where the key output proteins displayed adaptive resistance dynamics. Using these model instances, we next wanted to explore whether there were shared network features driving resistance, or if each model instance was unique in its ability to generate resistance. To explore this in a systematic manner, we extracted subsets of model instances, one for each key output protein and resistance behaviour combination (i.e. protein-dynamic combination) and performed a series of analyses on their parameters.

First, we investigated the mean and standard deviation of each parameter in each protein-dynamic combination to see if there were any individual parameter values underpinning resistance. We found that the mean of most parameters was between 0.1 and 1, but the standard deviation usually spanned 6 orders of magnitude (supplementary Figure S5). We did observe that all three receptor-activation associated parameters (kc1f1-INSR, kc10f1-FGFR, kc15f1-ER) were generally much lower in value than the rest, but further investigation ruled that this was generally due to higher values causing the model's system of ODEs to become too stiff, and therefore unsolvable, and were thus filtered out. We then undertook hierarchical clustering of each protein-dynamic combination's parameter values to try and identify if there were groups of parameter values driving resistance. However, we were unable to find any meaningful clusters (supplementary Figure S6). Together, these results led us to conclude that there were no particular individual parameters or groups of parameter values that were responsible for driving resistance.

Having found no patterns in the raw, or absolute, parameter values, we decided to investigate how frequently each parameter contributed to the increase or recovery of protein activity following drug perturbation, for each output protein. To this end, we investigated the effects of parameter knockdowns on the following dynamic features: maximum concentration, final concentration and/or rebound, hereafter collectively referred to as 'resistance features'. These features were chosen as they represent either an increase or recovery of protein activity, post drug perturbation, that could potentially enable a cell to overcome the drug insult. The relevant resistance features for biphasic and increasing dynamics were maximum concentration and final concentration, and the relevant features for rebound dynamics were rebound and final concentration. Rebound is not applicable to biphasic and increasing dynamics as it simply hasn't occurred, and the maximum concentration is only applicable to rebounding dynamics if the rebound overshoots the initial concentration, which is then covered by final concentration.

To measure the influence of parameters on the resistance features of the key output proteins we performed a high-throughput perturbation analysis wherein we reduced the value of each parameter by 20% in the third simulation phase i.e. the drug treatment phase. Parameters were perturbed one parameter at a time, and we measured the effect on the output protein's resistance features. A breakdown of the measured dynamic features, including the resistance features just described, is given in supplementary Figure S7.

If the knockdown of a parameter resulted in a reduction in the resistance features of the output proteins' dynamic, it scored a 1; otherwise it scored a 0. Repeating this process for each parameter and model instance resulted in an M x N matrix, where M is the number of model instances (protein and dynamic dependent), and N is the number of perturbed parameters (94), for each protein-dynamic combination. See Figure 5A for a visual representation of this, and the remaining overall process.

Initially, we wanted to determine how frequently each parameter contributed to the resistance features of each output protein. To achieve this, we summed up the number of times a parameter scored a 1 in the preceding analysis across all model instances, for each protein-dynamic combination. The results were plotted as bar graphs (top and bottom 10 parameters), which can be seen in supplementary Figure S8. The graphs showed clear rankings in how frequently each parameter contributed to the adaptive resistance features of each protein dynamic. Each protein-dynamic combination displayed a unique ranking but there also appeared to be a significant overlap in the top-scoring parameters. There also appeared to be more intra-protein overlap than inter-protein overlap, and pppRb and CDK2cycE shared much more similarity with each other than either with pRb. It was also interesting to observe that for biphasic pppRb and CDK2cycE, their top-scoring parameters accounted for approximately 90% of all model instances, indicating that these parameters must be critical in driving this particular dynamic for these proteins. The remaining top scoring parameters for each protein-dynamic subset only accounted for between 50-80% of model instances, suggesting each protein-dynamic combination possesses a degree of heterogeneity in the parameters that drive their adaptive resistance dynamics.

Together, the above results show that it is not the value of individual parameters that drive adaptive resistance, but rather it is the manner in which parameters co-ordinate to shape the quantitative and qualitative features of a protein's dynamic that drives adaptive resistance.

MDN can identify a full spectrum of core sub-networks that facilitate resistance

The observation that the top-scoring parameters generally do not broadly drive adaptive resistance dynamics suggests that there may be a number of different network states that are capable of driving a given resistance dynamic. To investigate this possibility, we subjected the matrices produced in the previous analysis to hierarchical clustering to try and find groups of model instances with shared resistance-driving parameter signatures. As a prime example, we first focused on rebounding hyperphosphorylation of Rb; both as the hyperphosphorylation of Rb strongly promotes cell cycle progression, and because previous studies have demonstrated the role of this protein-dynamic combination in CDK4/6 inhibitor resistance (21, 53, 54). Figure 5B displays a heatmap showing how rebounding pppRb model instances cluster, with respect to the contribution of their parameters to the rebounding dynamic.

The clustering of the pppRb-rebound model instances produced 9 robust clusters, where robust clusters are defined as those that contain at least 1% of the total protein-dynamic combination model instances, and the top-scoring parameter in the cluster accounts for at least 80% of its constituent model instances. Simply put, the clusters accounted for a high enough proportion of the model instances and the top scoring parameter was robustly representative of the model instances within the cluster. The left-most column of the heatmap in Figure 5C shows the overall ranking for how frequently each parameter contributes to the rebound dynamic of pppRb, and the remaining 9 columns represent the 9 clusters, aligned with the overall ranking. We observed a fairly strong consensus amongst the top-scoring parameters, with the majority of the cluster

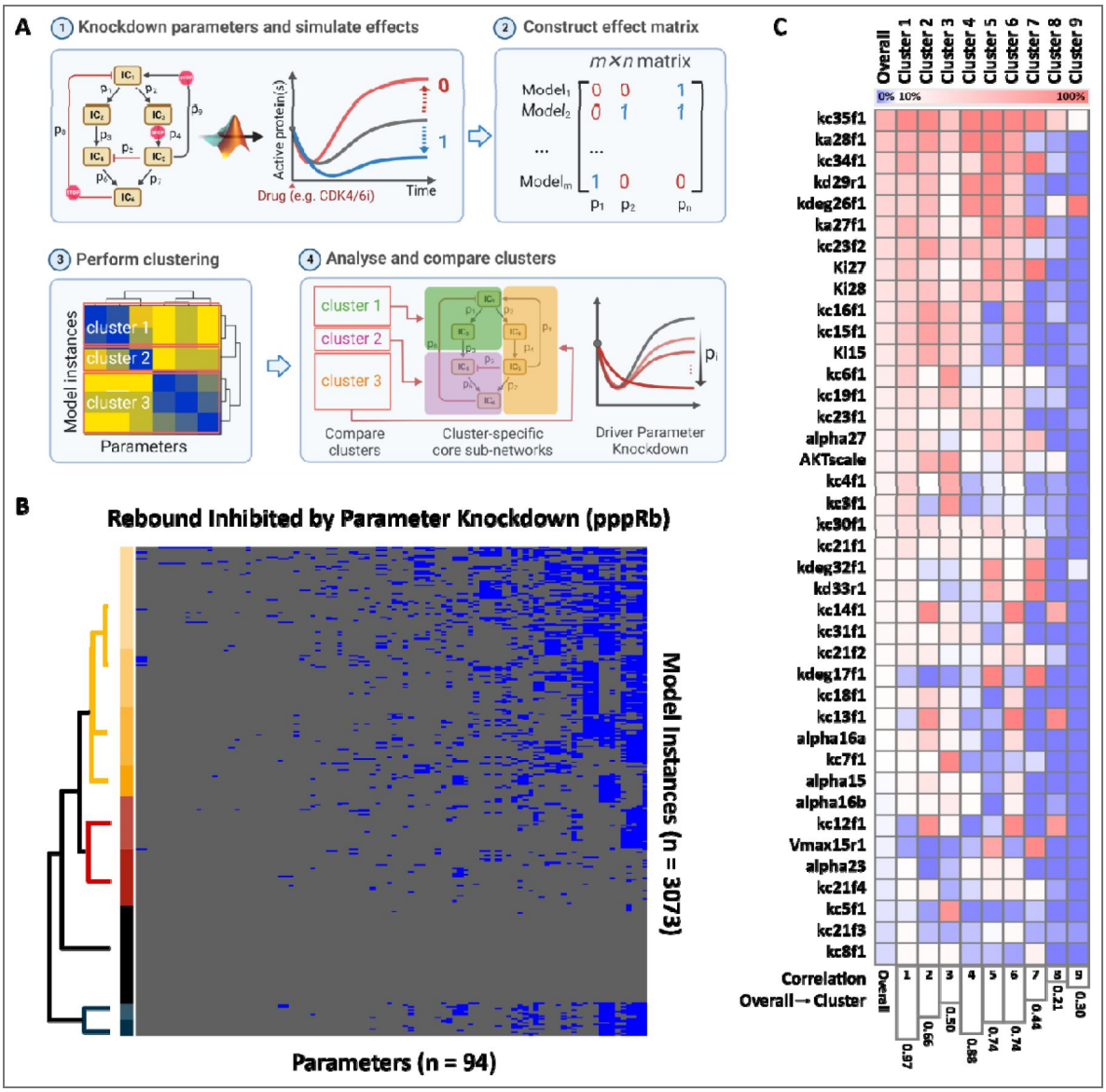

Figure 5. MDN analysis identifies core sub-networks that facilitate resistance.

A) Overview of the process undertaken to investigate the relationship between parameter knockdown and resistance-dynamic features to identify resistance driving parameter signatures. Each parameter is knocked down by 20%, one at a time, and the effect on the protein dynamics is measured. If the knockdown decreases resistance it scores a 1, otherwise it scores a 0. This process is repeated for each parameter, one at a time, for each model instance. The end result is a matrix where the columns represent parameters, and the rows represent the model instances. This matrix can then be analysed using clustering methods to identify parametric resistance signatures. **B)** Heatmap produced by hierarchical clustering of the parameters that contribute to rebounding pppRb, for model instances that display rebounding pppRb. **C)** Comparing parametric resistance signatures with the parameters that most frequently contribute to resistance overall. Parameters are ranked by how frequently they contribute to rebounding pppRb. Clusters are aligned with overall ranking. The lower bar graph represents the correlation between the overall ranking and each cluster specific ranking. This heatmap shows that some parametric resistance signatures align closely with the overall ranking, but some clusters are quite different, emphasising the context specificity of resistance.

differences coming from the middle and lower parameters (Figure 5C). Of note, this pattern appeared to be broadly true when we analysed all the 9 protein-dynamic groups (supplementary Figure S9).

Despite broad similarities between the clusters, many of the individual clusters did not correlate particularly well with the overall ranking and possessed clear differences in their resistance-driving parameter signatures (Figure 5C). These results suggest that the same drug response dynamic for the same protein in two different cells can be driven by different network states. To highlight the similarities and differences between the subnetworks underpinning resistance driven by pppRb rebound, we overlayed the parameter signatures of the five largest clusters on the ECC network schematic (Figure 6A). This revealed significant overlap between the clusters around the formation of the CDK2-cyclin E complex and the hyperphosphorylation of Rb itself. These results were to be expected as the CDK2-cyclin E complex is directly responsible for the hyperphosphorylation of Rb and confirms the logical hypothesis that CDK2 activation can drive the reactivation of Rb phosphorylation following CDK4/6 and ER inhibition. However, that almost all of the clusters shared this core network suggests that this subnetwork alone is likely sufficient to enable the reactivation of Rb phosphorylation on its own and would be strongly selected for by cancer during treatment. Similarly, but less expectedly, we also found strong overlap at the level of Myc (Figure 6A), suggesting a strong likelihood for its involvement in the development of resistance.

On the other hand, clusters that have less overlap highlight potential differences in underlying resistance mechanisms between patients experiencing seemingly similar drug responses. For the pppRb-rebound group, these clusters included those driven by the PI3K and MAPK pathways, protein degradation regulation (GSK3B), and p21/27 inhibition of the CDK2-cyclin E complex (Figure 6A). Consistently, when we targeted (inhibited) parameters related to these signalling nodes across different clusters we did not observe universal suppression of pppRb; instead, we saw cluster-specific suppression of pppRb (Figure 6B).

Expanding this analysis to include all 9 protein-dynamic combinations, we observed that resistance-promoting subnetworks were widespread throughout the ECC network (supplementary Figure S10 and Figures S10A-I). Further, we identified just under 100 robust clusters/subnetworks capable of facilitating resistance dynamics (supplementary Table S2A – J). Finally, to highlight the overlap between protein-dynamic clusters, we combined all of the individual clusters of all of the protein-dynamic combinations (supplementary Figure S11).

This revealed resistance most frequently converges on the activation of CDK2. Mechanisms driving this activation include: the promotion of cyclin E synthesis, reduction in cyclin E degradation, promotion of the formation of the CDK2cyclin E complex and suppression of p21 and p27 mediated CDK2 inhibition. There were also moderate contributions to resistance spread throughout both upstream mitogenic pathways. The contribution of the ER to resistance seemed to be context dependent. A strong deactivation rate of the ER contributed to resistance quite frequently, yet paradoxically strong activation of the ER also somewhat frequently contributed.

The above results suggest three things. First, while there is a moderately large number of network states that can drive resistance to dual CDK4/6-ER inhibition, there is very likely only a **finite** number of network states that cancer can exploit to overcome drug perturbation.

Second, the moderately large number of network states that facilitate resistance and the observation that any given resistance dynamic can be driven by many different mechanisms highlight the low likelihood of finding broadly-applicable resistance mechanisms. Third, some protein nodes and interactions contribute far more frequently to resistance than others. It is quite possible that these frequencies are related to the likelihood and tumorigenicity of mutations affecting these nodes/interactions.

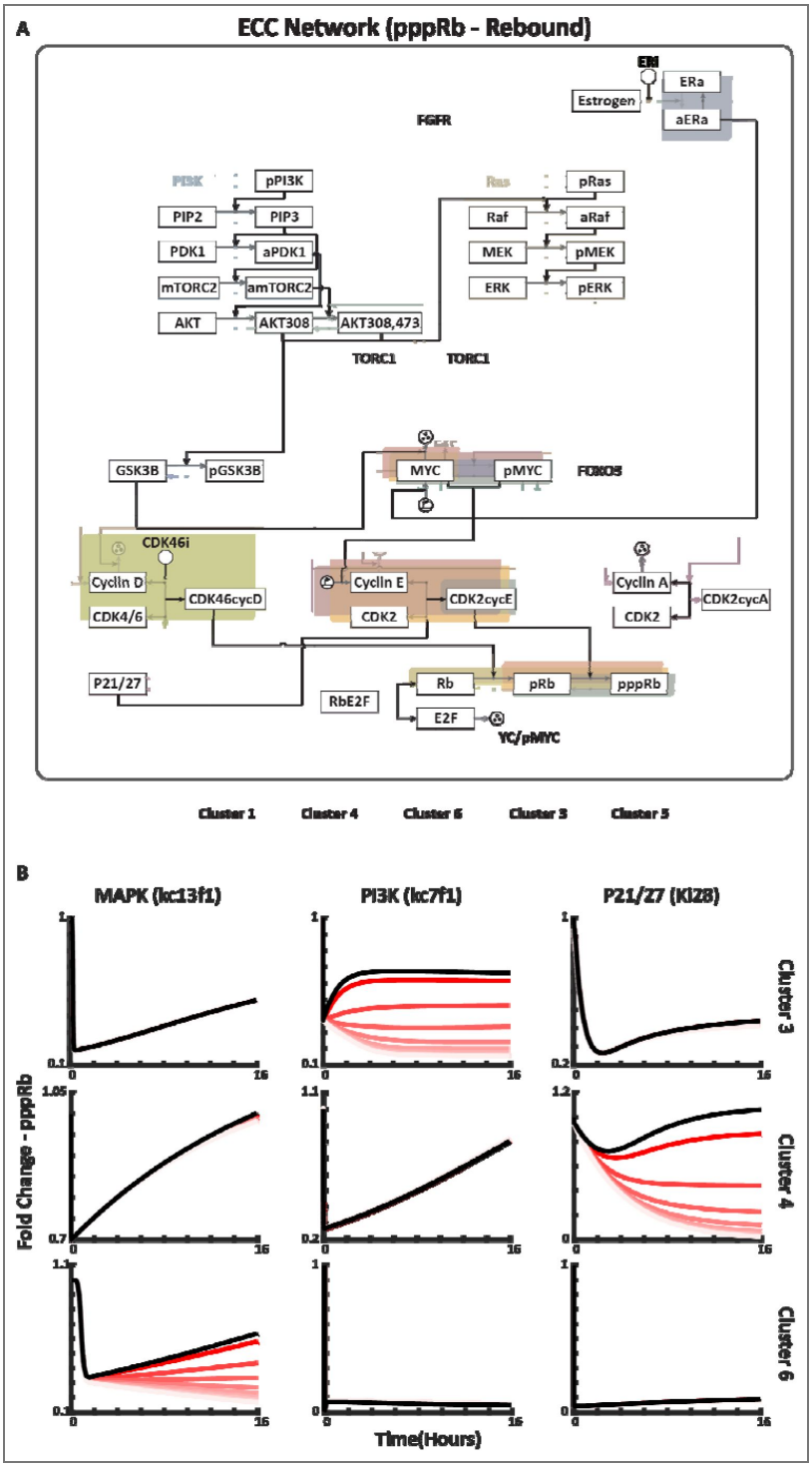

Figure 6. Identification of subnetworks driving pppRb rebound-mediated resistance within the ECC network.

A) Cluster-specific parameter signatures overlaid with the ECC network to highlight subnetworks that drive resistance through rebound of pppRb. Only the five largest clusters (out of 9) are displayed. **B)** Parameter knockdowns for the top-scoring parameters in three select clusters that display divergent resistance driving parameter signatures. Black represents treatment with CDK4/6 and ER inhibitors alone, decreasingly-red lines represent the addition of an increasingly potent parameter knockdown. These results highlight the context specificity of parameter knockdown when attempting to prevent adaptive resistance.

Qualitative support for MDN modelling-based simulations and predictions Monoculture cell populations demonstrate a significant degree of heterogeneous signalling dynamics in response to CDK4/6 inhibitors

This study provides a theoretical framework that connects heterogeneity, protein signalling dynamics and adaptive resistance mechanisms. To validate this framework, we analysed the literature to pinpoint biological evidence for a number of our key predictions. First, we wanted to observe if and how much drug-response signalling heterogeneity exists in cellular monocultures. Second, we wanted to find evidence that cells possess differential resistance-mediating subnetworks. And third, we wanted to determine if the resistance-mediating subnetworks we identified agree with known resistance mechanisms.

Recently, Yang et al. constructed a novel reporter system that enabled them to investigate the activity of CDK4/6 and CDK2 in individual MCF10A cells in response to three clinically approved CDK4/6 inhibitors: abemaciclib, palbociclib and ribociclib (55). Plotting the single-cell time-course data for each drug and protein revealed that, at the single-cell level, there is a wide variety of protein signalling dynamics (Figure 7A). We then subjected this time-course data to our category analysis to calculate the distribution of each protein's drug response dynamics (Figure 7B). We found that at the level of CDK4/6, the direct target of the three drugs, there was a moderate degree of signalling heterogeneity. Additionally, even the most potent drug (abemaciclib) failed to induce sustained suppression in approximately 10% of the cell population. The activity levels of CDK2, however, showed a much greater degree of signalling heterogeneity; and all three of the drugs only managed to strongly suppress CDK2 activity in a sustained manner in 40% of the population (Figure 7B). We further observed that there were many individual cells that demonstrated *increasing* CDK2 activity in response to CDK4/6 inhibition, a particularly unintuitive result, predicted by our MDN analysis. We then extracted a random sample of model instances from our MDN analysis (parametric variation) and plotted the drug response dynamics of CDK46cycD and CDK2cycE, our model's equivalent active forms of CDK4/6 and CDK2 (Figure 7C). The resemblance between the distribution of dynamics produced by our model simulations and the single-cell data is striking, both showing very similar proportions of resistant and sensitive dynamics.

Finally, we examined how the distribution of specific dynamics changed when comparing CDK4/6 activity with CDK2 activity. Figure 7D shows that the single-cell data and our MDN analysis exhibit the same general trends: there are more resistant dynamics at the level of CDK2 than at the level of CDK4/6; there are fewer sensitive dynamics at the level of CDK2 than CDK4/6; and there are more increasing dynamics at the level of CDK2. Perhaps most unintuitively, there are fewer rebound dynamics at the level of CDK2 in the single cell data, which was also predicted by our MDN analysis. Though this analysis is *qualitative*, we demonstrate the capacity for variation in protein activity within a conserved network architecture to drive a wide variety of signalling dynamics, including those associated with resistance, that mirrors the variation in signalling dynamics seen in isogenic single cells.

The identified resistance-mediating core subnetworks align with known resistance mechanisms

Previous studies have identified a wealth of mechanisms responsible for driving resistance to CDK4/6 and ER inhibitors. Focusing on mechanisms that have overlap with our model, the vast majority of identified mechanisms align quite well with the predictions made by our MDN analysis, validating the ability of this technique to identify a full spectrum of resistance-driving mechanisms. Moreover, our analysis also makes predictions about additional protein nodes/interactions that have not yet been identified by the literature.

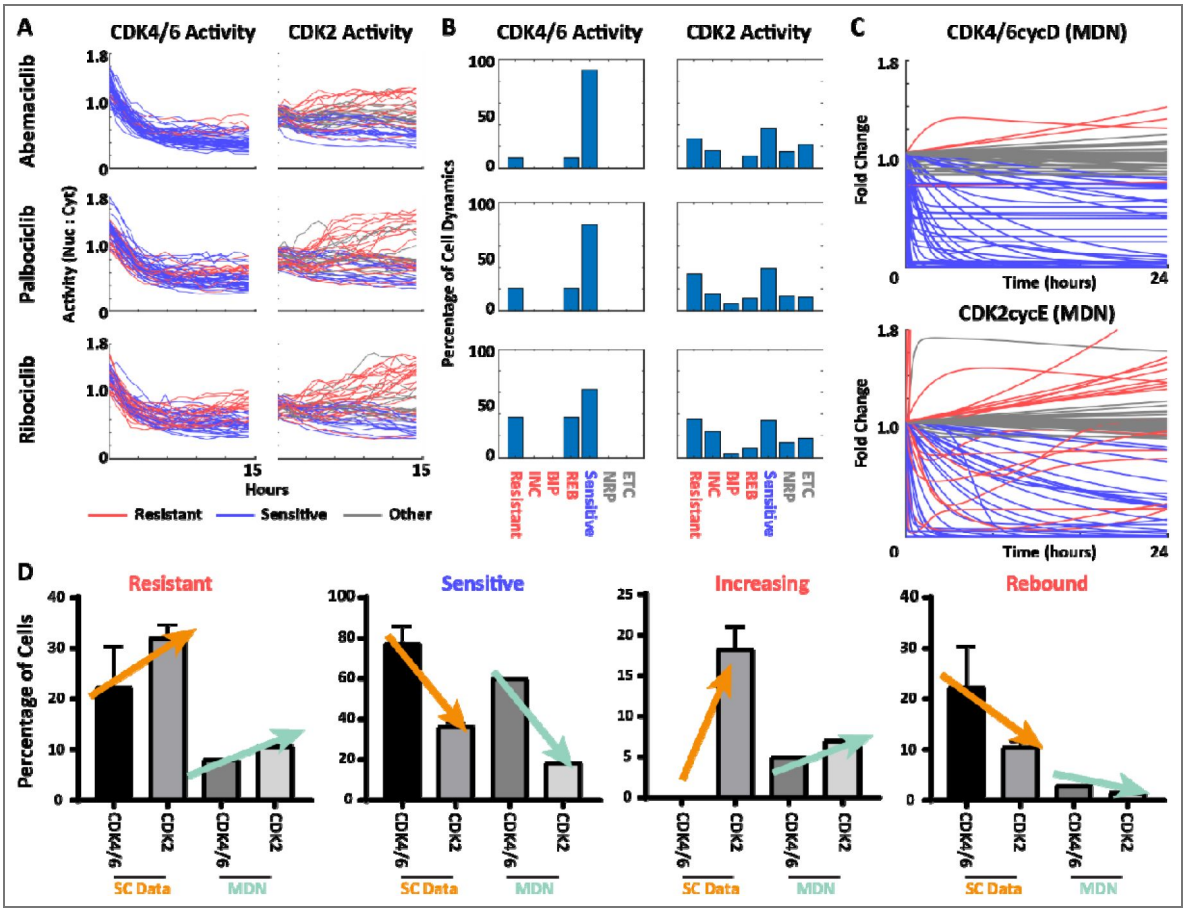

Figure 7. Validation of MDN-based predictions.

Qualitative comparisons between single-cell data and our MDN analyses. **A)** Single-cell time-course responses to CDK4/6 inhibition from Yang et al. (55)). The reporter readout reflects phosphorylation-dependent nucleo-cytoplasmic shuttling; the y-axis is the nuclear/cytoplasmic fluorescence ratio (not fold-change to t=0). Baseline values at t=0 therefore vary across cells (typically ~1–1.8) due to inherent differences in reporter localization prior to treatment. Red traces: resistance-associated dynamics; blue: sensitivity-associated; grey: no/limited response. **B)** Frequency of each dynamic category in panel A. **C)** Representative MDN simulations for CDK4/6·CycD and CDK2·CycE drawn from the model ensemble (parametric variation). Colours denote the same dynamic classes as in A. The distribution of resistant and sensitive dynamics from our simulations are highly correlated with the single-cell data. **D)** Agreement between single-cell data and MDN simulations quantified by the distribution of dynamic classes across both datasets.

Known mechanisms of resistance to CDK4/6 inhibitors include: Rb loss/mutations (56, 57), CDK4/6 overexpression (58–60), loss of ER expression (58, 61, 62), loss of PTEN (63), reduced expression/activity of p21 and p27 (64–66), activation of mTOR complexes (67, 68), activation of PI3K and PI3K signalling pathways (61, 69), activation of PDK1 (70), upregulation of FGFR (71, 72), AKT amplification and/or over-activation (73), E2F amplification and/or over-activation (74), MAPK pathway activation (75–77), c-Myc activity (78, 79), cyclin E overexpression and increased CDK2-cyclin E complex formation (43, 44, 80, 81). Known mechanisms of resistance to ER inhibitors include mutations that induce the constitutive activation of ER (82, 83), loss of ER activity (84, 85), activation of PI3K and MAPK signalling (86, 87), overexpression of c-Myc (88, 89) and loss of p21 and p27 (90, 91).

The preceding list represents a wealth of known resistance mechanisms that are widely distributed throughout the ECC network. Every single one of the above mechanisms is represented in at least one of our identified resistance-driving subnetworks. To clearly demonstrate how well our MDN analysis captured the known resistance mechanisms we created a table containing the known resistance mechanisms and the respective resistance-driving parameters identified by our MDN analysis (supplementary Table S3). The ability of MDN to largely capture the known resistance mechanisms highlights its potential usefulness in predicting resistance mechanisms to novel drugs and drug targets. Apart from capturing the known resistance mechanisms, our analysis really extends the observation that resistance can emerge from many different nodes within the ECC network and further adds support to the idea that it is critical to treat each patient individually.

Discussion

Heterogeneity is a defining feature of cancer and a major barrier to durable responses to targeted therapies. Clinical and experimental studies of CDK4/6 inhibitors in ER+ breast cancer consistently show wide inter- and intra-tumour variability in response and multiple, often co-existing resistance mechanisms (92). Yet, despite this wealth of descriptive data, we still lack mechanistic frameworks that can systematically relate underlying molecular heterogeneity to the spectrum of signalling behaviours that enable adaptive drug resistance. In this work, we introduce meta-dynamic network (MDN) modelling as such a framework. By sampling broad ensembles of kinetic parameters and protein abundances on a fixed network topology, MDN maps the full distribution of qualitative signalling dynamics ('meta-dynamics') accessible to a network architecture, and identifies which of these trajectories are compatible with sustained target inhibition versus adaptive escape.

Our first key finding is that even within a single, fixed early cell-cycle (ECC) network topology, variation in reaction kinetics and total protein abundances can generate a surprisingly rich repertoire of qualitative signalling behaviours. We use the term 'meta-dynamics' to denote the convergent distribution of these behaviours across a large ensemble of model instances, which represents a theoretical upper limit on what the network can manifest dynamically.

Importantly, this repertoire includes trajectories in which continuous CDK4/6 inhibition fails to maintain target suppression and downstream cell-cycle arrest - canonical signatures of adaptive resistance. This provides a concrete mechanistic link between molecular heterogeneity and the well-described phenomenon of rapid signalling rewiring under targeted therapy, in which feedback and crosstalk restore pathway activity despite continued drug exposure (18, 93).

We find that adaptive resistance can emerge from heterogeneity in both kinetic parameters and protein abundances, but not symmetrically. However, across the ECC network, we observe that perturbations to kinetic parameters (interaction strengths) are more potent and consistent drivers of adaptive resistance dynamics than changes in total protein abundance. This supports a hierarchical view of control: network topology and interaction strengths largely determine which qualitative behaviours are possible, while protein levels modulate how frequently particular regimes are accessed. That hierarchy is consistent with both systems-level perspectives on cellular

heterogeneity (94) and parameter-sensitivity analyses in whole-cell and signalling models, which have shown that many distinct parameter sets can collapse onto a limited set of functional outputs (95).

Perhaps the most striking observation from our analysis is how rapidly the meta-dynamic distribution converges. Despite sweeping over 90 kinetic parameters and 50 total abundances across nine orders of magnitude, the distribution of qualitative response classes stabilises well before 100,000 accepted model instances. Doubling the ensemble size yields only negligible changes in the frequencies of each dynamic regime, see supplementary Figure S12. This reflects a strong filtering effect imposed by network topology rather than simply a statistical inevitability of sampling from fixed priors. When parameters or abundances are pushed to extremes, nodes tend to be driven into saturating states, either effectively 'always off' or 'always on', and become unresponsive to upstream perturbations. These saturated cases fall into the 'no response' category and do not generate new, more complex temporal patterns. Consequently, the ECC topology funnels the near-infinite combinatorial parameter space into a finite, recurring set of qualitative behaviours (e.g. monotonic decrease, rebound, biphasic).

Such topology-constrained behavioural repertoires have also been noted in recent work that treats heterogeneity by assigning probability distributions to model parameters and analysing the resulting ensemble of single-cell behaviours (96, 97). MDN complements these approaches by emphasising qualitative dynamic classes and their frequencies rather than precise parameter posteriors.

At the level of individual nodes and subnetworks, our perturbation analyses reveal that adaptive resistance is a genuinely network-level property. Nearly every node in the ECC model can be implicated in at least one resistance subnetwork when viewed across the full heterogeneity ensemble, echoing the clinical and experimental literature where numerous, sometimes mutually exclusive mechanisms of CDK4/6 inhibitor resistance have been described - ranging from loss of RB1, to cyclin E/CDK2 activation, PI3K–AKT upregulation, FGFR signalling, and alterations in cell-cycle checkpoint control (92). However, MDN does not predict an unstructured 'anything goes' landscape. When we rank interactions by how frequently their perturbation participates in resistance-associated trajectories, a small set of hubs and co-regulated modules emerges. In other words, many routes to resistance exist, but they tend to be coordinated through a limited number of recurrent network motifs and subnetworks. This modular picture is consistent with reviews of adaptive resistance in breast cancer, which emphasise convergent rewiring of signalling hubs and feedback nodes despite diverse upstream lesions (18).

As an additional, orthogonal validation of the resistance subnetworks identified by MDN, we compared our perturbation-derived resistance modules with gene-dependency patterns from the Cancer Dependency Map (DepMap) (98). Although DepMap is not specific to CDK4/6 inhibition, hierarchical clustering of knockout dependencies for ECC-network genes revealed distinct vulnerability modules across >1000 cell lines (supplementary Figure S13). The existence of such modules supports the MDN prediction that different cellular contexts rely on distinct but recurrent subnetworks to sustain proliferation, reinforcing the view that resistance is governed by coordinated network-level processes rather than isolated nodes.

Our findings also shed light on why CDK4/6 inhibition resistance is so pervasive yet difficult to capture with single biomarkers. Recent work integrating bulk, single-cell, and trial data has shown that tumours resistant to CDK4/6 inhibition are characterised by increased intra-tumoural heterogeneity and multiple, co-existing resistance signatures, including MYC-driven programmes and altered estrogen-response pathways (99). Single-cell imaging and modelling studies have further demonstrated that cell-cycle dynamics and signalling trajectories at the single-cell level are critical determinants of CDK4/6 inhibitor sensitivity (100). Our MDN analysis provides a mechanistic underpinning for these observations: across a broad space of plausible network states, a surprisingly large fraction of configurations yield adaptive resistance-like signalling for key G1-S regulators, and simultaneous durable suppression of all relevant downstream effectors is

rare. In such a landscape, static measurements of one or a few nodes are unlikely to robustly stratify patients, because resistance is inherently encoded in distributed, dynamic network behaviour rather than in single static markers.

Despite the theoretical nature of our study, qualitative comparison with single-cell signalling data supports the core results of MDN. Experiments in isogenic breast epithelial cells have shown that CDK4/6 activity reporters display highly heterogeneous dynamics under inhibitor treatment, with some cells remaining durably suppressed, others partially rebounding, and others showing minimal inhibition (55, 100). Our meta-dynamic distributions reproduce this spectrum of behaviours despite being generated from a much broader parameter ensemble than any one cell line is likely to occupy. We emphasise that this comparison is intentionally qualitative: our goal is not to fit a specific cell line with a calibrated model, but to demonstrate that the ECC topology, when subjected to realistic heterogeneity, naturally gives rise to the types of signalling trajectories observed empirically. The close qualitative agreement between simulated and experimental distributions suggests that even nominally isogenic populations may explore a substantial portion of the network's meta-dynamic landscape.

As with any model-based framework, MDN has limitations that shape how its predictions should be interpreted. First, we use mass-action and first-order kinetics rather than more detailed Michaelis–Menten or cooperative rate laws. This was essential to keep the parameter space tractable for large-scale exploration, but it means that behaviours relying critically on enzyme saturation or higher-order cooperativity may be under-represented. Second, our parameter and abundance priors are deliberately broad and largely uniform in log-space, whereas biochemical parameters and expression levels in real cells are often better approximated by log-normal or other structured distributions (101–103). In this sense, the present work should be viewed as defining what is possible for a given topology rather than estimating what is probable in a specific tumour context. Third, our model is deterministic and does not explicitly capture intrinsic biochemical noise. We argue that sampling across a broad ensemble of parameter and abundance sets can approximate the time-averaged consequences of genetic, epigenetic, and stochastic variation, but intrinsic noise at low copy numbers and rare event dynamics will require explicit stochastic formulations (104). Finally, the ECC model abstracts some multi-protein modules into single nodes to maintain computational tractability. As a result, highly ranked "hub" nodes in our analysis should be interpreted as implicating critical processes or modules, rather than single gene products, as the key levers of resistance.

These limitations point naturally to several avenues for future work. A priority is to constrain MDN ensembles using experimentally inferred parameter and abundance distributions, for example by integrating Bayesian parameter-inference methods that represent cell-to-cell variability as probability distributions over model parameters. Another key direction is to couple MDN-derived resistance subnetworks with data-driven approaches that operate directly on patient-derived single-cell and spatial multi-omics data, which are increasingly used to dissect sample-level heterogeneity and its association with treatment response (105). Such integrated frameworks could bridge the gap between mechanistic prediction of resistance-enabling subnetworks and empirical identification of patient-specific vulnerabilities. On the dynamical side, embedding stochastic simulations or Langevin approximations within the MDN framework would allow us to evaluate how intrinsic noise reshapes the meta-dynamic landscape and whether it introduces qualitatively new resistance regimes or primarily modulates the frequencies of existing ones. Finally, our perturbation analyses suggest that a finite set of recurrent resistance modules underpins a vast number of resistant states. This aligns with translational efforts that design rational combination therapies to pre-empt or overcome adaptive resistance by co-targeting signalling hubs and compensatory feedbacks (106) and MDN could provide a principled way to enumerate and prioritise such combinations for experimental testing.

In summary, MDN modelling offers a systems-level framework that connects molecular heterogeneity to dynamic signalling behaviour and, ultimately, to adaptive drug resistance. By revealing how a fixed network topology can generate a finite but diverse set of resistance-associated trajectories, and by identifying the hubs and modules that recurrently mediate these

trajectories, our work complements empirical single-cell and clinical studies and suggests concrete strategies for network-level intervention. Although we have focused on the G1-S transition and CDK4/6 inhibition as a clinically important case study, the MDN approach is broadly applicable to other signalling networks and therapeutic targets. As mechanistic models, single-cell datasets, and computational methods continue to mature, we envisage MDN-like frameworks playing an increasingly important role in predicting how tumours will escape targeted treatments and in guiding combination strategies to keep them one step ahead.

Data availability

We did not generate data for this manuscript.

Acknowledgements

L.K.N was funded by a Victorian Cancer Agency Mid-Career Research Fellowship (MCRF18026); a Venture Grant from Cancer Council Victoria, Australia; and an Investigator Initiated Research grant from the National Breast Cancer Foundation and Love Your Sister, Australia (IIRS-20–094). A.H was This research is/was supported by an Australian Government Research Training Program (RTP) Scholarship. This research was supported in part by the Australian Research Council Centre of Excellence for the Mathematical Analysis of Cellular Systems (MACSYS, CE230100001), funded by the Australian Government.

Additional information

Author contributions

Conceptualization: Anthony Hart, Lan K. Nguyen.

Formal analysis: Anthony Hart, Sung-Young Shin, Lan K. Nguyen. Funding acquisition: Lan K. Nguyen.

Project administration: Lan K. Nguyen. Supervision: Lan K. Nguyen.

Writing – original draft: Anthony Hart, Lan K. Nguyen, Sung-Young Shin.

Author ORCID iDs

Anthony Hart: https://orcid.org/0000-0003-1557-6515
Sung-Young Shin: https://orcid.org/0000-0002-1447-9687
Lan K Nguyen: https://orcid.org/0000-0003-4040-7705

Additional files

Model File 1

Model File 2

Model File 3

Model File 4

Supplementary Table 1

Supplementary Table 2

Supplementary Table 3

Supplementary Information

References

1. **Vasan N,** Baselga J, Hyman DM (2019) A view on drug resistance in cancer. *Nature* **575**:299-309
2. **Wang X,** Zhang H, Chen X (2019) Drug resistance and combating drug resistance in cancer. *Cancer Drug Resistance* **2**:141

3. **Pich O,** Bailey C, Watkins TB, Zaccaria S, Jamal-Hanjani M, Swanton C (2022) The translational challenges of precision oncology. *Cancer Cell*
4. **Knudsen ES,** Kumarasamy V, Nambiar R, Pearson JD, Vail P, Rosenheck H, Wang J, Eng K, Bremner R, Schramek D, *et al.* (2022) CDK/cyclin dependencies define extreme cancer cell-cycle heterogeneity and collateral vulnerabilities. *Cell Reports* **38**:110448
5. **Jubran MR,** Vilenski D, Flashner-Abramson E, Shnaider E, Vasudevan S, Rubinstein AM, Meirovitz A, Sharon S, Polak D, Kravchenko-Balasha N (2022) Overcoming resistance to EGFR monotherapy in HNSCC by identification and inhibition of individualized cancer processes. *Theranostics* **12**:1204-1219
6. **Dagogo-Jack I,** Shaw AT (2018) Tumour heterogeneity and resistance to cancer therapies. *Nat Rev Clin Oncol* **15**:81-94
7. **Turke AB,** Zejnullahu K, Wu Y-L, Song Y, Dias-Santagata D, Lifshits E, Toschi L, Rogers A, Mok T, Sequist L (2010) Preexistence and clonal selection of MET amplification in EGFR mutant NSCLC. *Cancer cell* **17**:77-88
8. **Patel AG,** Chen X, Huang X, Clay MR, Komorova N, Krasin MJ, Pappo A, Tillman H, Orr BA, McEvoy J (2022) The myogenesis program drives clonal selection and drug resistance in rhabdomyosarcoma. *Developmental Cell* **57**:1226-1240.e8
9. **Cassidy J.** (2019) Studying the clonal origins of drug resistance in human breast cancers. University of Cambridge.
10. **Herrera-Abreu MT,** Palafox M, Asghar U, Rivas MA, Cutts RJ, Garcia-Murillas I, Pearson A, Guzman M, Rodriguez O, Grueso J, *et al.* (2016) Early Adaptation and Acquired Resistance to CDK4/6 Inhibition in Estrogen Receptor-Positive Breast Cancer. *Cancer Res* **76**:2301-13
11. **Ahmed TA,** Adamopoulos C, Karoulia Z, Wu X, Sachidanandam R, Aaronson SA, Poulikakos PI (2019) SHP2 Drives Adaptive Resistance to ERK Signaling Inhibition in Molecularly Defined Subsets of ERK-Dependent Tumors. *Cell Rep* **26**:65-78.
12. **Blombery P,** Anderson MA, Gong JN, Thijssen R, Birkinshaw RW, Thompson ER, Teh CE, Nguyen T, Xu Z, Flensburg C, *et al.* (2019) Acquisition of the Recurrent Gly101Val Mutation in BCL2 Confers Resistance to Venetoclax in Patients with Progressive Chronic Lymphocytic Leukemia. *Cancer Discov* **9**:342-353
13. **Yun CH,** Mengwasser KE, Toms AV, Woo MS, Greulich H, Wong KK, Meyerson M, Eck MJ (2008) The T790M mutation in EGFR kinase causes drug resistance by increasing the affinity for ATP. *Proc Natl Acad Sci U S A* **105**:2070-5
14. **Xue X,** Liang X-J (2012) Overcoming drug efflux-based multidrug resistance in cancer with nanotechnology. *Chinese journal of cancer* **31**:100
15. **Smyth MJ,** Krasovskis E, Sutton VR, Johnstone RW (1998) The drug efflux protein, P-glycoprotein, additionally protects drug-resistant tumor cells from multiple forms of caspase-dependent apoptosis. *Proceedings of the National Academy of Sciences* **95**:7024-7029
16. **Jin X,** Ge LP, Li DQ, Shao ZM, Di GH, Xu XE, Jiang YZ. (2020) LncRNA TROJAN promotes proliferation and resistance to CDK4/6 inhibitor via CDK2 transcriptional activation in ER+ breast cancer. *Mol Cancer* **19**:87
17. **Li Q,** Jiang B, Guo J, Shao H, Del Priore IS, Chang Q, Kudo R, Li Z, Razavi P, Liu B, *et al.* (2022) INK4 Tumor Suppressor Proteins Mediate Resistance to CDK4/6 Kinase Inhibitors. *Cancer Discov* **12**:356-371
18. **Cremers CG,** Nguyen LK (2019) Network rewiring, adaptive resistance and combating strategies in breast cancer. *Cancer Drug Resistance* **2**:1106
19. **Wright SCE,** Vasilevski N, Serra V, Rodon J, Eichhorn PJA (2021) Mechanisms of resistance to PI3K inhibitors in cancer: adaptive responses, drug tolerance and cellular plasticity. *Cancers* **13**:1538
20. **Ma P,** Fu Y, Chen M, Jing Y, Wu J, Li K, Shen Y, Gao J-X, Wang M, Zhao X (2016) Adaptive and acquired resistance to EGFR inhibitors converge on the MAPK pathway. *Theranostics* **6**:1232

21. **Herrera-Abreu MT,** Palafox M, Asghar U, Rivas MA, Cutts RJ, Garcia-Murillas I, Pearson A, Guzman M, Rodriguez O, Grueso J (2016) Early Adaptation and Acquired Resistance to CDK4/6 Inhibition in Estrogen Receptor–Positive Breast CancerEarly Adaption and Acquired Palbociclib Resistance. *Cancer research* **76**:2301-2313

22. **Park S-M,** Hwang CY, Choi J, Joung CY, Cho K-H (2020) Feedback analysis identifies a combination target for overcoming adaptive resistance to targeted cancer therapy. *Oncogene* **39**:3803-3820

23. **Nguyen LK,** Kholodenko BN (2016) Feedback regulation in cell signalling: Lessons for cancer therapeutics. *Seminars in Cell & Developmental Biology* **50**:85-94

24. **Bachmann J,** Raue A, Schilling M, Becker V, Timmer J, Klingmüller U (2012) Predictive mathematical models of cancer signalling pathways. *Journal of Internal Medicine* **271**:155-165

25. **Shankar E,** Weis MC, Avva J, Shukla S, Shukla M, Sreenath SN, Gupta S (2019) Complex Systems Biology Approach in Connecting PI3K-Akt and NF-κB Pathways in Prostate Cancer. *Cells* **8**:201

26. **Clarke MA,** Fisher J (2020) Executable cancer models: successes and challenges. *Nature Reviews Cancer* **20**:343-354

27. **Altrock PM,** Liu LL, Michor F (2015) The mathematics of cancer: integrating quantitative models. *Nature Reviews Cancer* **15**:730-745

28. **Ghomlaghi M,** Hart A, Hoang N, Shin S, Nguyen LK (2021) Feedback, crosstalk and competition: ingredients for emergent non-linear behaviour in the PI3K/mTOR signalling network. *International journal of molecular sciences* **22**:6944

29. **Tyson JJ,** Laomettachit T, Kraikivski P (2019) Modeling the dynamic behavior of biochemical regulatory networks. *Journal of theoretical biology* **462**:514-527

30. **Tandon G,** Yadav S, Kaur S (2022) Chapter 24 - Pathway modeling and simulation analysis. In: Singh DB, Pathak RK (Eds). *Bioinformatics* Academic Press. pp. 409-423 https://doi.org/10.1016/B978-0-323-89775-4.00007-9

31. **Deuflhard P,** Röblitz S (2015) ODE Models for Systems Biological Networks. In: Deuflhard P, Röblitz S (Eds). *A Guide to Numerical Modelling in Systems Biology* Cham: Springer International Publishing. pp. 1-32 https://doi.org/10.1007/978-3-319-20059-0_1

32. **Kearney AL,** Norris DM, Ghomlaghi M, Wong MKL, Humphrey SJ, Carroll L, Yang G, Cooke KC, Yang P, Geddes TA (2021) Akt phosphorylates insulin receptor substrate to limit PI3K-mediated PIP3 synthesis. *eLife* **10**:e66942 https://doi.org/10.7554/eLife.66942

33. **Shin SY,** Müller AK, Verma N, Lev S, Nguyen LK (2018) Systems modelling of the EGFR-PYK2-c-Met interaction network predicts and prioritizes synergistic drug combinations for triple-negative breast cancer. *PLoS Comput Biol* **14**:e1006192

34. **Sun X,** Hu B (2017) Mathematical modeling and computational prediction of cancer drug resistance. *Briefings in Bioinformatics* **19**:1382-1399

35. **Chisholm RH,** Lorenzi T, Clairambault J (2016) Cell population heterogeneity and evolution towards drug resistance in cancer: biological and mathematical assessment, theoretical treatment optimisation. *Biochimica et Biophysica Acta (BBA)-General Subjects* **1860**:2627-2645

36. **Belkhir S,** Thomas F, Roche B (2021) Darwinian approaches for cancer treatment: benefits of mathematical modeling. *Cancers* **13**:4448

37. **Huang B,** Jia D, Feng J, Levine H, Onuchic JN, Lu M (2018) RACIPE: a computational tool for modeling gene regulatory circuits using randomization. *BMC Syst Biol* **12**:74

38. **Städter P,** Schälte Y, Schmiester L, Hasenauer J, Stapor PL (2021) Benchmarking of numerical integration methods for ODE models of biological systems. *Scientific Reports* **11**:2696

39. **Resat H,** Petzold L, Pettigrew MF (2009) Kinetic modeling of biological systems. *Methods Mol Biol* **541**:311-35

40. **Stallaert W,** Kedziora KM, Taylor CD, Zikry TM, Ranek JS, Sobon HK, Taylor SR, Young CL, Cook JG, Purvis JE (2022) The structure of the human cell cycle. *Cell Systems* **13**:230-240.

41. **Tyson JJ,** Novák B (2015) Models in biology: lessons from modeling regulation of the eukaryotic cell cycle. *BMC Biology* **13**:46

42. **Iorio F,** Knijnenburg TA, Vis DJ, Bignell GR, Menden MP, Schubert M, Aben N, Gonçalves E, Barthorpe S, Lightfoot H, *et al.* (2016) A Landscape of Pharmacogenomic Interactions in Cancer. *Cell* **166**:740-754

43. **Min A,** Kim JE, Kim YJ, Lim JM, Kim S, Kim JW, Lee KH, Kim TY, Oh DY, Bang YJ, *et al.* (2018) Cyclin E overexpression confers resistance to the CDK4/6 specific inhibitor palbociclib in gastric cancer cells. *Cancer Lett* **430**:123-132

44. **Taylor-Harding B,** Aspuria PJ, Agadjanian H, Cheon DJ, Mizuno T, Greenberg D, Allen JR, Spurka L, Funari V, Spiteri E, *et al.* (2015) Cyclin E1 and RTK/RAS signaling drive CDK inhibitor resistance via activation of E2F and ETS. *Oncotarget* **6**:696-714

45. **Ahmed TA,** Adamopoulos C, Karoulia Z, Wu X, Sachidanandam R, Aaronson SA, Poulikakos PI (2019) SHP2 drives adaptive resistance to ERK signaling inhibition in molecularly defined subsets of ERK-dependent tumors. *Cell reports* **26**:65-78.e5

46. **Chen J,** Bai M, Ning C, Xie B, Zhang J, Liao H, Xiong J, Tao X, Yan D, Xi X (2016) Gankyrin facilitates follicle-stimulating hormone-driven ovarian cancer cell proliferation through the PI3K/AKT/HIF-1α/cyclin D1 pathway. *Oncogene* **35**:2506-2517

47. **Wang H-Y,** Yang S-L, Liang H-F, Li C-H (2014) HBx protein promotes oval cell proliferation by up-regulation of cyclin D1 via activation of the MEK/ERK and PI3K/Akt pathways. *International journal of molecular sciences* **15**:3507-3518

48. **Del Re M,** Crucitta S, Lorenzini G, De Angelis C, Diodati L, Cavallero D, Bargagna I, Cinacchi P, Fratini B, Salvadori B. (2021) PI3K mutations detected in liquid biopsy are associated to reduced sensitivity to CDK4/6 inhibitors in metastatic breast cancer patients. *Pharmacological Research* **163**:105241

49. **Samuels Y,** Velculescu VE (2004) Oncogenic mutations of PIK3CA in human cancers. *Cell cycle* **3**:1221-1224

50. **FDA** (2017) Palbociclib (IBRANCE). FDA. https://www.fda.gov/drugs/resources-information-approved-drugs/palbociclib-ibrance#:~:text=FDA%20granted%20palbociclib%20accelerated%20approval,based%20therapy%20in%20postmenopausal%20women

51. **FDA** (2017) Ribociclib (Kisqali). FDA. https://www.fda.gov/drugs/resources-information-approved-drugs/ribociclib-kisqali

52. **FDA** (2021) FDA approves abemaciclib with endocrine therapy for early breast cancer. FDA. https://www.fda.gov/drugs/resources-information-approved-drugs/fda-approves-abemaciclib-endocrine-therapy-early-breast-cancer

53. **Kim S,** Leong A, Kim M, Yang HW (2022) CDK4/6 initiates Rb inactivation and CDK2 activity coordinates cell-cycle commitment and G1/S transition. *Sci Rep* **12**:16810

54. **Narasimha AM,** Kaulich M, Shapiro GS, Choi YJ, Sicinski P, Dowdy SF (2014) Cyclin D activates the Rb tumor suppressor by mono-phosphorylation. *eLife* **3**

55. **Yang HW,** Cappell SD, Jaimovich A, Liu C, Chung M, Daigh LH, Pack LR, Fan Y, Regot S, Covert M, *et al.* (2020) Stress-mediated exit to quiescence restricted by increasing persistence in CDK4/6 activation. *eLife* **9**:e44571 https://doi.org/10.7554/eLife.44571

56. **Malorni L,** Piazza S, Ciani Y, Guarducci C, Bonechi M, Biagioni C, Hart CD, Verardo R, Di Leo A, Migliaccio I. (2016) A gene expression signature of retinoblastoma loss-of-function is a predictive biomarker of resistance to palbociclib in breast cancer cell lines and is prognostic in patients with ER positive early breast cancer. *Oncotarget* **7**:68012-68022

57. **Palafox M,** Monserrat L, Bellet M, Villacampa G, Gonzalez-Perez A, Oliveira M, Brasó-Maristany F, Ibrahimi N, Kannan S, Mina L. (2022) High p16 expression and heterozygous RB1 loss are biomarkers for CDK4/6 inhibitor resistance in ER+ breast cancer. *nature communications* **13**:1-20

58. **Yang C,** Li Z, Bhatt T, Dickler M, Giri D, Scaltriti M, Baselga J, Rosen N, Chandarlapaty S (2017) Acquired CDK6 amplification promotes breast cancer resistance to CDK4/6 inhibitors and loss of ER signaling and dependence. *Oncogene* **36**:2255-2264

59. **Li Z,** Razavi P, Li Q, Toy W, Liu B, Ping C, Hsieh W, Sanchez-Vega F, Brown DN, Paula AFDC (2018) Loss of the FAT1 tumor suppressor promotes resistance to CDK4/6 inhibitors via the hippo pathway. *Cancer cell* **34**:893-905.e8

60. **Olanich ME,** Sun W, Hewitt SM, Abdullaev Z, Pack SD, Barr FG (2015) CDK4 Amplification Reduces Sensitivity to CDK4/6 Inhibition in Fusion-Positive Rhabdomyosarcoma. *Clin Cancer Res* **21**:4947-59

61. **Takeshita T,** Yamamoto Y, Yamamoto-Ibusuki M, Tomiguchi M, Sueta A, Murakami K, Iwase H. (2018) Clinical significance of plasma cell-free DNA mutations in PIK3CA, AKT1, and ESR1 gene according to treatment lines in ER-positive breast cancer. *Mol Cancer* **17**:67

62. **Iida M,** Toyosawa D, Nakamura M, Tsuboi K, Tokuda E, Niwa T, Ishida T, Hayashi SI (2020) Decreased ER dependency after acquired resistance to CDK4/6 inhibitors. *Breast Cancer* **27**:963-972

63. **Costa C,** Wang Y, Ly A, Hosono Y, Murchie E, Walmsley CS, Huynh T, Healy C, Peterson R, Yanase S (2020) PTEN loss mediates clinical cross-resistance to CDK4/6 and PI3Kα inhibitors in breast cancer. *Cancer discovery* **10**:72-85

64. **Kumarasamy V,** Vail P, Nambiar R, Witkiewicz AK, Knudsen ES (2021) Functional Determinants of Cell Cycle Plasticity and Sensitivity to CDK4/6 Inhibition. *Cancer Research* **81**:1347-1360

65. **Patel P,** Tsiperson V, Gottesman SRS, Somma J, Blain SW (2018) Dual Inhibition of CDK4 and CDK2 via Targeting p27 Tyrosine Phosphorylation Induces a Potent and Durable Response in Breast Cancer Cells. *Mol Cancer Res* **16**:361-377

66. **Iida M,** Nakamura M, Tokuda E, Toyosawa D, Niwa T, Ohuchi N, Ishida T, Hayashi SI (2019) The p21 levels have the potential to be a monitoring marker for ribociclib in breast cancer. *Oncotarget* **10**:4907-4918

67. **Michaloglou C,** Crafter C, Siersbaek R, Delpuech O, Curwen JO, Carnevalli LS, Staniszewska AD, Polanska UM, Cheraghchi-Bashi A, Lawson M, *et al.* (2018) Combined Inhibition of mTOR and CDK4/6 Is Required for Optimal Blockade of E2F Function and Long-term Growth Inhibition in Estrogen Receptor-positive Breast Cancer. *Mol Cancer Ther* **17**:908-920

68. **Goel S,** Wang Q, Watt AC, Tolaney SM, Dillon DA, Li W, Ramm S, Palmer AC, Yuzugullu H, Varadan V, *et al.* (2016) Overcoming Therapeutic Resistance in HER2-Positive Breast Cancers with CDK4/6 Inhibitors. *Cancer Cell* **29**:255-269

69. **O'Brien NA,** McDermott MS, Conklin D, Luo T, Ayala R, Salgar S, Chau K, DiTomaso E, Babbar N, Su F (2020) Targeting activated PI3K/mTOR signaling overcomes acquired resistance to CDK4/6-based therapies in preclinical models of hormone receptor-positive breast cancer. *Breast Cancer Research* **22**:1-17

70. **Jansen VM,** Bhola NE, Bauer JA, Formisano L, Lee KM, Hutchinson KE, Witkiewicz AK, Moore PD, Estrada MV, Sánchez V, *et al.* (2017) Kinome-Wide RNA Interference Screen Reveals a Role for PDK1 in Acquired Resistance to CDK4/6 Inhibition in ER-Positive Breast Cancer. *Cancer Res* **77**:2488-2499

71. **Turner N,** Pearson A, Sharpe R, Lambros M, Geyer F, Lopez-Garcia MA, Natrajan R, Marchio C, Iorns E, Mackay A, *et al.* (2010) FGFR1 amplification drives endocrine therapy resistance and is a therapeutic target in breast cancer. *Cancer Res* **70**:2085-94

72. **Formisano L,** Lu Y, Servetto A, Hanker AB, Jansen VM, Bauer JA, Sudhan DR, Guerrero-Zotano AL, Croessmann S, Guo Y, *et al.* (2019) Aberrant FGFR signaling mediates resistance to CDK4/6 inhibitors in ER+ breast cancer. *Nature Communications* **10**:1373

73. **Alves CL,** Ehmsen S, Terp MG, Portman N, Tuttolomondo M, Gammelgaard OL, Hundebøl MF, Kaminska K, Johansen LE, Bak M, *et al.* (2021) Co-targeting CDK4/6 and AKT with endocrine therapy prevents progression in CDK4/6 inhibitor and endocrine therapy-resistant breast cancer. *Nature Communications* **12**:5112

74. **Dean JL,** Thangavel C, McClendon AK, Reed CA, Knudsen ES (2010) Therapeutic CDK4/6 inhibition in breast cancer: key mechanisms of response and failure. *Oncogene* **29**:4018-4032

75. **Hayes TK,** Luo F, Cohen O, Goodale AB, Lee Y, Pantel S, Bagul M, Piccioni F, Root DE, Garraway LA, *et al.* (2019) A Functional Landscape of Resistance to MEK1/2 and CDK4/6 Inhibition in NRAS-Mutant Melanoma. *Cancer Research* **79**:2352-2366

76. **De Leeuw R,** McNair C, Schiewer MJ, Neupane NP, Brand LJ, Augello MA, Li Z, Cheng LC, Yoshida A, Courtney SM. (2018) MAPK Reliance via Acquired CDK4/6 Inhibitor Resistance in CancerCDK4/6 Inhibitor Resistance in Cancer. *Clinical Cancer Research* **24**:4201-4214

77. **Haines E,** Chen T, Kommajosyula N, Chen Z, Herter-Sprie GS, Cornell L, Wong K-K, Shapiro GI (2018) Palbociclib resistance confers dependence on an FGFR-MAP kinase-mTOR-driven pathway in KRAS-mutant non-small cell lung cancer. *Oncotarget* **9**:31572

78. **Mo H,** Liu X, Xue Y, Chen H, Guo S, Li Z, Wang S, Li C, Han J, Fu M, *et al.* (2022) S6K1 amplification confers innate resistance to CDK4/6 inhibitors through activating c-Myc pathway in patients with estrogen receptor-positive breast cancer. *Molecular Cancer* **21**:171

79. **Robinson AM,** Rathore R, Redlich NJ, Adkins DR, VanArsdale T, Van Tine BA, Michel LS. (2019) Cisplatin exposure causes c-Myc-dependent resistance to CDK4/6 inhibition in HPV-negative head and neck squamous cell carcinoma. *Cell death & disease* **10**:1-13

80. **Pandey K,** Park N, Park K-S, Hur J, Cho YB, Kang M, An H-J, Kim S, Hwang S, Moon YW (2020) Combined CDK2 and CDK4/6 inhibition overcomes palbociclib resistance in breast cancer by enhancing senescence. *Cancers* **12**:3566

81. **Hall CR,** Bisi JE, Strum JC (2019) Inhibition of CDK2 overcomes primary and acquired resistance to CDK4/6 inhibitors. *Cancer Research* **79**:4414-4414

82. **Jeselsohn R,** Yelensky R, Buchwalter G, Frampton G, Meric-Bernstam F, Gonzalez-Angulo AM, Ferrer-Lozano J, Perez-Fidalgo JA, Cristofanilli M, Gomez H (2014) Emergence of Constitutively Active Estrogen Receptor-α Mutations in Pretreated Advanced Estrogen Receptor–Positive Breast CancerESR1-Activating Mutations in Advanced Breast Cancer. *Clinical cancer research* **20**:1757-1767

83. **Masri S,** Phung S, Wang X, Wu X, Yuan Y-C, Wagman L, Chen S (2008) Genome-wide analysis of aromatase inhibitor-resistant, tamoxifen-resistant, and long-term estrogen-deprived cells reveals a role for estrogen receptor. *Cancer research* **68**:4910-4918

84. **Vesuna F,** Lisok A, Kimble B, Domek J, Kato Y, van der Groep P, Artemov D, Kowalski J, Carraway H, van Diest P. (2012) Twist contributes to hormone resistance in breast cancer by downregulating estrogen receptor-α. *Oncogene* **31**:3223-3234

85. **Johnston S,** Saccani-Jotti G, Smith I, Salter J, Newby J, Coppen M, Ebbs S, Dowsett M (1995) Changes in estrogen receptor, progesterone receptor, and pS2 expression in tamoxifen-resistant human breast cancer. *Cancer research* **55**:3331-3338

86. **Miller TW,** Hennessy BT, González-Angulo AM, Fox EM, Mills GB, Chen H, Higham C, García-Echeverría C, Shyr Y, Arteaga CL (2010) Hyperactivation of phosphatidylinositol-3 kinase promotes escape from hormone dependence in estrogen receptor-positive human breast cancer. *J Clin Invest* **120**:2406-13

87. **Campbell RA,** Bhat-Nakshatri P, Patel NM, Constantinidou D, Ali S, Nakshatri H (2001) Phosphatidylinositol 3-kinase/AKT-mediated activation of estrogen receptor α: a new model for anti-estrogen resistance. *Journal of Biological Chemistry* **276**:9817-9824

88. **McNeil CM,** Sergio CM, Anderson LR, Inman CK, Eggleton SA, Murphy NC, Millar EK, Crea P, Kench JG, Alles MC (2006) . c-Myc overexpression and endocrine resistance in breast cancer. *The Journal of steroid biochemistry and molecular biology* **102**:147-155

89. **Planas-Silva MD,** Bruggeman RD, Grenko RT, Smith J (2007) Overexpression of c-Myc and Bcl-2 during progression and distant metastasis of hormone-treated breast cancer. *Experimental and molecular pathology* **82**:85-90

90. **Abukhdeir AM,** Vitolo MI, Argani P, De Marzo AM, Karakas B, Konishi H, Gustin JP, Lauring J, Garay JP, Pendleton C. (2008) Tamoxifen-stimulated growth of breast cancer due to p21 loss. *Proceedings of the National Academy of Sciences* **105**:288-293

91. **Massarweh S,** Osborne CK, Jiang S, Wakeling AE, Rimawi M, Mohsin SK, Hilsenbeck S, Schiff R (2006) Mechanisms of tumor regression and resistance to estrogen deprivation and fulvestrant in a model of estrogen receptor–positive, HER-2/neu-positive breast cancer. *Cancer research* **66**:8266-8273

92. **Zhou FH,** Downton T, Freelander A, Hurwitz J, Caldon CE, Lim E (2023) CDK4/6 inhibitor resistance in estrogen receptor positive breast cancer, a 2023 perspective. *Frontiers in Cell and Developmental Biology* **11**

93. **Chandarlapaty S** (2012) Negative Feedback and Adaptive Resistance to the Targeted Therapy of Cancer. *Cancer Discovery* **2**:311-319

94. **Movasat H,** Giacopino E, Shahdoost A, Dorri Nokoorani Y, Abrbekouh AH, Tahamtani Y, Shakiba N (2025) A systems view of cellular heterogeneity: Unlocking the "wheel of fate". *Cell Syst* **16**:101300

95. **Babtie AC,** Stumpf MPH (2017) How to deal with parameters for whole-cell modelling. *Journal of The Royal Society Interface* **14**

96. **Yamada T,** Nishiyama M, Oba S, Jimbo HC, Ikeda K, Ishii S, Hong K, Sakumura Y (2018) Computational Methods for Estimating Molecular System from Membrane Potential Recordings in Nerve Growth Cone. *Scientific Reports* **8**:4559

97. **Spencer SL,** Gaudet S, Albeck JG, Burke JM, Sorger PK (2009) Non-genetic origins of cell-to-cell variability in TRAIL-induced apoptosis. *Nature* **459**:428-432

98. **Ghandi M,** Huang FW, Jané-Valbuena J, Kryukov GV, Lo CC, McDonald ER, Barretina J, Gelfand ET, Bielski CM, Li H (2019) Next-generation characterization of the cancer cell line encyclopedia. *Nature* **569**:503-508

99. **Migliaccio I,** Bonechi M, Romagnoli D, Boccalini G, Galardi F, Guarducci C, Nardone A, Schiff R, Biganzoli L, Malorni L, *et al.* (2025) Single-cell transcriptomics reveals biomarker heterogeneity linked to CDK4/6 Inhibitor resistance in breast cancer cell lines. *npj Breast Cancer* **11**:82

100. **Asghar US,** Barr AR, Cutts R, Beaney M, Babina I, Sampath D, Giltnane J, Lacap JA, Crocker L, Young A, *et al.* (2017) Single-Cell Dynamics Determines Response to CDK4/6 Inhibition in Triple-Negative Breast Cancer. *Clin Cancer Res* **23**:5561-5572

101. **Taniguchi Y,** Choi PJ, Li GW, Chen H, Babu M, Hearn J, Emili A, Xie XS (2010) Quantifying E. coli proteome and transcriptome with single-molecule sensitivity in single cells. *Science* **329**:533-8

102. **Bar-Even A,** Milo R, Noor E, Tawfik DS (2015) The Moderately Efficient Enzyme: Futile Encounters and Enzyme Floppiness. *Biochemistry* **54**:4969-77

103. **Bengtsson M,** Ståhlberg A, Rorsman P, Kubista M (2005) Gene expression profiling in single cells from the pancreatic islets of Langerhans reveals lognormal distribution of mRNA levels. *Genome Res* **15**:1388-92

104. **Kwon T,** Kwon O-S, Cha H-J, Sung BJ (2019) Stochastic and Heterogeneous Cancer Cell Migration: Experiment and Theory. *Scientific Reports* **9**:16297

105. **Boyeau P,** Hong J, Gayoso A, Kim M, McFaline-Figueroa JL, Jordan MI, Azizi E, Ergen C, Yosef N (2025) Deep generative modeling of sample-level heterogeneity in single-cell genomics. *Nature Methods* **22**:2264-2274

106. **Yip HYK,** Shin SY, Chee A, Ang CS, Rossello FJ, Wong LH, Nguyen LK, Papa A (2024) Integrative modeling uncovers p21-driven drug resistance and prioritizes therapies for PIK3CA-mutant breast cancer. *NPJ Precis Oncol* **8**:20

Peer reviews

Joint Public Review:

In this manuscript, the authors proposed an approach to systematically characterise how heterogeneity in a protein signalling network affects its emergent dynamics, with particular emphasis on drug-response signalling dynamics in cancer treatments. They named this approach Meta Dynamic Network (MDN) modelling, as it aims to consider the potential dynamic responses globally, varying both initial conditions (i.e., expression levels) and biophysical parameters (i.e., protein interaction parameters). By characterising the "meta" response of the network, the authors propose that the method can provide insights not only into the possible dynamic behaviours of the system of interest but also into the likelihood and frequency of observing these dynamic behaviours in the natural system.

The authors study the Early Cell Cycle (ECC) network as a proof of concept, focusing on pathways involving PI3K, EGFR, and CDK4/6 with the aim of identifying mechanisms that may underlie resistance to CDK4/6 inhibition in cancer. The biochemical reaction model comprises 50 state variables and 94 kinetic parameters, implemented in SBML and simulated in Matlab. A central component of the study is the generation of large ensembles of model instances, including 100,000 randomly sampled parameter sets intended to represent intra-tumour heterogeneity. On the basis of these simulations, the authors conclude that heterogeneity in kinetic rate parameters plays a stronger role in driving adaptive resistance than variation in baseline protein expression levels, and that resistance emerges as a network-level property rather than from individual components alone. The revised manuscript provides additional clarification regarding aspects of the simulation and filtering procedures and frames the comparison with experimental data as qualitative. Nonetheless, the study is best interpreted as a theoretical and exploratory analysis of the model's behaviour under heterogeneous conditions. Consequently, questions remain regarding the biological grounding of the sampled parameter regimes and the extent to which the reported frequencies of resistance-associated behaviours can be directly interpreted in physiological terms.

While the authors propose a potentially useful computational framework to explore how heterogeneity shapes dynamic responses to drug perturbation, a number of important conceptual and methodological concerns remain to be addressed:

(1) The sampling of kinetic parameters constitutes the backbone of the manuscript, yet important concerns remain regarding its biological grounding and transparency. Although the revised version provides additional clarification on the exploration of "model instances", it is still not sufficiently clear how parameter values and initial conditions are generated, nor how the chosen ranges relate to biological measurements. The kinetic rates are sampled over broad intervals without explicit justification in terms of experimentally measured bounds or inferred distributions. As a consequence, it remains uncertain whether the ensemble of simulated behaviours reflects physiologically plausible cellular regimes or primarily the properties of the assumed parameter space. In this context, the large-scale sampling (100,000 parameter sets) resembles a Monte Carlo exploration of the model rather than a biologically calibrated representation of tumour heterogeneity.

Furthermore, the adequacy of the sampling strategy in such a high-dimensional space (94 free parameters) remains open to question. In the absence of biologically informed constraints, the combinatorial space of possible parameter configurations is vast, and it is unclear to what extent the sampled ensembles can be considered representative. This issue is particularly relevant because the manuscript interprets the frequency of resistance-associated behaviours as indicative of their likelihood.

The validation presented in Figure 7 does not fully resolve these concerns. The comparison with experimental data is qualitative, and the simulations are performed in arbitrary time units, which complicates direct interpretation alongside time-resolved experimental measurements. Moreover, certain qualitative discrepancies between simulated and experimental trends (e.g., persistent versus decreasing CDK4/6 activity) are not thoroughly discussed. As this figure represents the primary empirical reference point in the manuscript, the extent to which the model captures experimentally observed dynamics remains uncertain.

Finally, aspects of presentation continue to limit transparency. Parameter ranges are described at different points in the manuscript but are not consolidated clearly in the Methods, and the definition of initial conditions remains ambiguous - particularly whether these correspond to conserved quantities or to the dynamic variables used to initialise simulations. In addition, the exact number of model instances underlying specific analyses and figures is not always explicit. Greater clarity on these issues is essential for assessing reproducibility and for interpreting the quantitative claims of the study.

(2) A central conclusion of the manuscript is that heterogeneity in protein-protein interaction kinetics is a stronger driver of adaptive resistance than heterogeneity in protein expression levels. To assess the latter, the authors fix a nominal set of kinetic parameters and generate 100,000 random initial concentrations for the 50 model species. However, according to the simulation protocol described in the manuscript, each trajectory includes three phases: (i) simulation under starvation conditions to equilibrium, (ii) mitogenic stimulation to a second ("fed") equilibrium, and (iii) application of drug treatment. The equilibrium concentrations reached in phases (i) and (ii) are determined by the kinetic parameters of the model and are independent of the initial concentrations, provided the system converges to a stable steady state. In dynamical systems terms, stable equilibria are defined by the parameter set and attract all initial conditions within their basin of attraction. Since the kinetic parameters are fixed in this experiment, the pre-treatment equilibrium that serves as the starting point for drug application should likewise be fixed. Under these conditions, it is therefore not unexpected that sampling a large number of initial concentrations has limited influence on the treated dynamics.

This raises conceptual questions about the interpretation of the comparison between kinetic and expression heterogeneity. If the system converges to a unique stable steady state prior to treatment, then variability in initial concentrations does not propagate into variability in drug response, and the observed dominance of kinetic heterogeneity may partly reflect this structural property of the model rather than a biological principle. Clarification is needed regarding whether multiple steady states exist under the nominal parameter set, and if so, how basins of attraction are explored.

More broadly, it remains unclear why initial protein concentrations can be sampled independently of the kinetic parameters. In biological systems, steady-state expression levels are typically determined by the underlying kinetic rates. A more consistent approach might require constraining initial concentrations to correspond to equilibrium states of the chosen parameter set, thereby introducing relationships between at least some of the 50 initial conditions and the 94 kinetic parameters. Finally, the manuscript employs a non-standard terminology regarding "initial conditions," which may further obscure interpretation of these results and would benefit from clarification.

(3) The technical implementation of the modelling and simulation framework remains difficult to evaluate due to insufficient methodological detail. Although the authors state that kinetic parameters are randomly sampled, the manuscript does not specify the distributions from which parameters are drawn, nor whether potential correlations between parameters are considered or explicitly ignored. Without this information, it is not possible to assess how implicit modelling assumptions shape the ensemble of simulated behaviours. Given that the

conclusions rely on frequency-based interpretations across sampled parameter sets, greater transparency regarding the sampling procedure is essential.

A further concern relates to the parameter filtering step. The authors report that the "vast majority" of sampled parameter sets produced systems that were "too stiff," and that these were excluded on the grounds that stiff dynamics are not biologically plausible. However, the manuscript does not clearly define how stiffness is assessed, nor why stiffness is interpreted as biologically unrealistic rather than as a numerical property of the formulation. In standard practice, stiff systems are typically handled using appropriate implicit solvers rather than being discarded. Similarly, parameter sets that produce negative state values are excluded, yet such behaviour may arise from numerical artefacts rather than from intrinsic model inconsistency. The rationale for excluding these parameter sets, rather than adapting the numerical scheme, is not sufficiently justified.

The reported rejection rate - approximately 90% of sampled parameter sets - is substantial and raises questions regarding the interplay between model structure, parameter ranges, and numerical methods. As currently described, the filtering step appears to select parameter sets based primarily on computational tractability rather than on experimentally motivated biological criteria. The manuscript would be strengthened by clarifying whether the retained parameter sets are representative of biologically meaningful regimes, and by distinguishing clearly between exclusions based on biological plausibility and those arising from numerical considerations.

Finally, important aspects of the simulation protocol require clarification. The model is simulated under "fasted" and "fed" conditions until equilibrium is reached, yet the criterion used to determine convergence is not specified. It would be important to describe how equilibrium is assessed (e.g., based on the norm of the time derivatives). Additionally, it remains unclear whether the mitogenic stimulus applied in the "fed" phase is assumed to be constant over time and, if so, how this assumption relates to biological experimental conditions. Greater detail on these implementation choices is necessary to ensure interpretability and reproducibility.

(4) The manuscript states that the modelling conclusions are strongly supported by existing literature; however, the validation presented does not fully substantiate this claim. As noted above, the comparison with CDK2 and CDK4/6 experimental data remains qualitative, and the use of arbitrary simulation time units complicates interpretation of temporal agreement. The extent to which the model quantitatively or mechanistically recapitulates experimentally observed dynamics therefore remains uncertain.

The claim that the model reproduces known resistance mechanisms is also difficult to assess in light of Figure S10, where a large fraction of network nodes (~80%) appear implicated in resistance under some conditions. If most components of the network can, in at least some parameter regimes, be associated with resistance phenotypes, the resulting lack of selectivity weakens the strength of model-based validation. It becomes challenging to distinguish specific mechanistic insights from generic consequences of network connectivity.

In addition, the Supplementary Information notes that certain components of the mitogenic and cell-cycle pathways were abstracted or excluded in order to maintain computational tractability. While such abstraction is understandable in a large ODE framework, it raises interpretative questions. Proteins identified as potential resistance drivers within the model may, in some cases, represent aggregated or simplified pathway effects. Clarifying in the main text how such abstractions may influence the attribution of resistance mechanisms would strengthen the biological interpretation of the results.

Drug inhibition is central to the manuscript's conclusions. The revised version clarifies that inhibition is implemented as a fixed fractional modification of specific kinetic rate laws. This

abstraction is appropriate for exploring network-level responses, but it represents a stylised perturbation rather than a pharmacologically calibrated model of drug action. For full interpretability and reproducibility, the mathematical form of the modified rate laws, as well as the timing of inhibition relative to network equilibration, should be specified unambiguously. The biological implications of the findings depend critically on understanding this modelling choice.

The one-at-a-time perturbation analysis presented in Figure 5 provides an interpretable ranking of first-order control points across the ensemble and offers mechanistic insight into primary sensitivities of the network. However, many targeted therapies act on multiple components, and resistance frequently arises through combinatorial mechanisms. The reported rankings should therefore be interpreted as identifying primary influences under isolated perturbations, rather than as a comprehensive account of multi-target drug behaviour.

Overall, the manuscript succeeds in presenting a conceptual and exploratory framework for analysing how signalling network topology can shape the qualitative landscape of adaptive responses under heterogeneous kinetic conditions. Its principal contribution lies in establishing a systematic platform for large-scale in silico exploration. At the same time, the current limitations in biological calibration, parameter grounding, and validation constrain the extent to which the conclusions can be interpreted as predictive or quantitatively representative of specific tumour contexts. Addressing these issues would further strengthen the connection between the theoretical landscape described here and experimentally observed resistance dynamics.

https://doi.org/10.7554/eLife.87710.2.sa1

Author response:

The following is the authors' response to the original reviews.

> ***Joint Public Reviews:***
>
> *In this manuscript, the authors proposed an approach to systematically characterise how heterogeneity in a protein signalling network affects its emergent dynamics, with particular emphasis on drug-response signalling dynamics in cancer treatments. They named this approach Meta Dynamic Network (MDN) modelling, as it aims to consider the potential dynamic responses globally, varying both initial conditions (i.e., expression levels) and biophysical parameters (i.e., protein interaction parameters). By characterising the "meta" response of the network, the authors propose that the method can provide insights not only into the possible dynamic behaviours of the system of interest but also into the likelihood and frequency of observing these dynamic behaviours in the natural system.*
>
> *The authors studied the Early Cell Cycle (ECC) network as a proof of concept, specifically focusing on PI3K, EGFR, and CDK4/6, with particular interest in identifying the mechanisms that cancer could potentially exploit to display drug resistance. The biochemical reaction model consists of 50 equations (state variables) with 94 kinetic parameters, described using SBML and computed in Matlab. Based on the simulations, the authors concluded the following main points: a large number of network states can facilitate resistance, the individual biophysical parameters alone are insufficient to predict resistance, and adaptive resistance is an emergent property of the network. Finally, the authors attempt to validate the model's prediction that differential core sub-networks can drive drug resistance by comparing their observations with the knock-out information available in the literature. The authors identified subnetworks potentially responsible for drug resistance through the inhibition of individual pathways.*

Importantly, some concerns regarding the methodology are discussed below, putting in doubt the validity of the main claims of this work.

While the authors proposed a potentially useful computational approach to better understand the effect of heterogeneity in a system's dynamic response to a drug treatment (i.e., a perturbation), there are important weaknesses in the manuscript in its current form:

(1) It is unclear how the random parameter sets (i.e., model instances) and initial conditions are generated, and how this choice biases or limits the general conclusions for the case studied. Particularly, it is not evident how the kinetic rates are related to any biological data, nor if the parameter distributions used in this study have any biological relevance.

(2) Related to this problem, it is not clear whether the considered 100,000 random parameter samples sufficiently explore parameter space due to the combinatorial explosion that arises from having 94 free parameters, nor 100,000 random initial conditions for a system with 50 species (variables).

(3) Moreover, the authors filter out all the cases with stiff behaviour. This filtering step appears to select model parameters based on computational convenience, rather than biological plausibility.

(4) Also, it is not clear how exactly the drug effect is incorporated into the model (e.g., molecular inhibition?), nor how it is evaluated in the dynamic simulations (e.g., at the beginning of the simulation?). Moreover, in a complex network, the results may differ depending on whether the inhibition is applied from the start or after the network has reached a stable state.

(5) On the same line, the conclusions need to be discussed in the context of stability, particularly when evaluating the role of initial conditions. As stable steady states are determined by the model parameters, once again, the details of how the perturbation effect is evaluated on the simulation dynamics are critical to interpret the results.

(6) The presented validation of the model results (Fig. 7) is only qualitative, and the interpretation is not carefully discussed in the manuscript, particularly considering the comparison between fold-change responses without specifying the baseline states.

We thank the reviewers for their thoughtful and constructive comments. In response to their comments, we have undertaken a substantial revision to address all the comments, improve clarity, transparency, and robustness while preserving the paper's core contribution: a principled, scalable framework (MDN) for mapping how molecular heterogeneity and network architecture shape adaptive drug-response dynamics. At a high level, we clarified the study design and analysis goals, tightened definitions, and added methodological detail where it most advances interpretability. Importantly, these updates leave the analytical pipelines and major conclusions unchanged.

Conceptually, we now make explicit that our objective is coverage of the output space of qualitative dynamics supported by the network topology, not exhaustive enumeration of parameter space. To support this, we added a convergence analysis and clarified that "triplicates" refers to independent ensembles used to demonstrate reproducibility. We also refined how we describe and implement initial conditions (as conserved total abundances that encode expression heterogeneity) and reframed filtering as minimal numerical/feasibility checks, using rejection sampling to obtain the prespecified ensemble size. Solver choices and input modelling (constant step mitogen/drug) are now spelled out succinctly.

We expanded the model specification and rationale (complete reaction list with rate laws and brief biological justifications in the Supplement) and unified terminology throughout. Figures and legends have been overhauled for readability and accuracy, with missing labels added and ordering corrected. For validation, we clarified the nature of the single-cell reporter readout, improved Figure 7's presentation, and emphasised - consistent with our aims - that comparisons are qualitative.

Finally, we have rewritten the Discussion to centre on interpretation, implications, and connect our findings to the literature. It now: (i) frames MDN as a systems-level framework that links molecular heterogeneity to qualitative signalling "meta-dynamics" and adaptive escape under constant drug pressure; (ii) highlights two key findings: an asymmetry in control (interaction kinetics exert stronger, more consistent influence than protein abundance) and a topology-driven convergence whereby a vast parameter space funnels into a finite set of recurrent behaviours; (iii) shows that resistance is a network-level property, with many possible routes but a small set of recurrent hubs/modules dominating; and (iv) provides a qualitative alignment with single-cell reporter data while clarifying the intent and limits of that comparison. Moreover, we now explicitly discuss limitations (rate-law simplifications, broad priors, determinism, and modular abstractions) and outline next steps for future research, including data-constrained priors and stochastic extensions.

We believe these revisions materially strengthen the manuscript and fully address all the reviewers' comments. A detailed, point-by-point response follows.

> ***Joint Recommendations for the Authors:***
>
> *(1) It is confusing exactly what are the different sets evaluated in each cases, e.g. "generated 100,000 model instances, each with the same set of ICs but a unique set of randomly generated parameter values" (lines 299-300), "generated 100,000 model instances (in triplicate), each with the same set of 'nominal' parameter values (see supplementary Table S1), and a unique set of ICs, and repeated the analysis as performed previously" (lines 366-368), "combined the 1000 IC sets with each parameter set to create 1000 model instances" (lines 382-383), "repeated for 1000 parameter sets, allowing us to observe how frequently IC variation induced adaptive resistance independent of the chosen parameter set" (lines 386-387). A small table or just a clearer explanation is needed.*

In response to these comments, we have revised the main text to clarify the process of model instance generation. Specifically, we have made changes at page 7: line 297 - page 8: line 302, page 8: lines 305 - 310, page 9: lines 372-378, and page 9: line 384 – page 10: line 399 in the revised main text.

We have also added a new Figure (Figure S1) to the supplementary file to allow readers to visualise the model generation process for each relevant set of experiments. Supplementary figures are referenced in the main text where appropriate.

> *(2) The authors mentioned performing each simulation in triplicate, which is puzzling as the model is based on deterministic ODEs with fixed parameters for each simulation. Under such conditions, one would anticipate identical results from multiple simulations with the same initial conditions and fixed parameters. Perhaps the authors expect the model to exhibit chaos or aim to assess the precision of the parameter estimates through triplicate simulations. Further clarification from the authors would be valuable to comprehend the rationale behind conducting triplicate simulations in a deterministic setting.*

We agree that repeating deterministic ODE simulations with identical inputs would be redundant. In our study, "triplicate" referred instead to generating three independent

ensembles of 100,000 unique model instances each, where model parameters (or initial conditions) were randomly resampled. These ensembles were analysed separately to assess whether the inferred meta-dynamic distributions converged robustly. Indeed, the distributions from the three replicates were nearly indistinguishable, confirming that the results are reproducible and not artefacts of a particular random draw.

We have revised the main text to clarify this distinction (page 8: lines 305 - 310) and added an extended explanation for meta-dynamic behaviour convergence in the new section Error Convergence in the supplementary text (page 6: lines 184 - 210).

> *(3) While the lack of a connection between model parameters and biological data (mentioned in the public review) may not be a fatal flaw in the manuscript, the concern about the 100,000 random samples being insufficient to explore the parameter space is valid. In a thought experiment, considering the high and low rate for each parameter and the combinatorial explosion of possibilities (2^94), the number of simulations performed (100,000) represents only an extremely small fraction of the entire parameter space (~1/10^(23)). This limitation might not accurately capture the true heterogeneity present inside a solid tumour. One potential solution is to determine biological bounds on model parameters through data fitting, which can provide more meaningful constraints for the simulations. Alternatively, increasing the number of simulations and adopting more efficient sampling techniques can enhance the coverage of possible parameter sets.*

We thank the reviewer for this insightful comment. We agree that the 94-dimensional parameter space is vast, and that 100,000 simulations represent only a fraction of the total combinatorial possibilities. However, the objective of our study is not to exhaustively sample the entire parameter space, but rather to sufficiently sample the 'output space' - that is, the complete spectrum of qualitative dynamic behaviours the network topology can generate. The key question is whether 100,000 model instances are sufficient for the distribution of these output dynamics to converge.

To formally address this, we have performed a convergence analysis, which is now detailed in the new supplementary section "Error Convergence" (Supplementary text page 6: lines 184 - 210) and illustrated in Supplementary Figure S12. This analysis demonstrates that the mean squared error (MSE) between dynamic distributions from N and 2N simulations exponentially decreases as N increases, and the distribution of protein dynamics changes negligibly well before reaching 100,000 instances. Furthermore, performing the entire analysis in triplicate with independent random seeds yielded nearly identical meta-dynamic maps (average standard deviation < 0.04%), giving us high confidence that we have robustly captured the network's behavioural repertoire.

We believe this convergence occurs because the system is degenerate: many distinct parameter sets within the high-dimensional space map to the same qualitative outcome (e.g., 'rebound' or 'decreasing'). Our goal was to capture the set of possible outcomes, not every unique parameter combination that leads to them.

Regarding the parameter range, we intentionally chose a broad, unbiased range (10^{-5} to 10)as a proof-of-concept to delineate the theoretical upper limit of heterogeneity the network can support, thereby capturing even rare but potentially critical resistance dynamics. We agree with the reviewer that a future direction is to constrain these ranges using biological data. Such an approach would transition from defining what is possible (the focus of this manuscript) to predicting what is probable in a specific biological context. We have added this important point to the Discussion (page 16: lines 663-679) to highlight this avenue for future work.

> *(4) One of the manuscript's main results indicates that protein interactions play a more significant role in driving adaptive resistance than protein expression. To explore the impact of protein expression, the authors fixed a nominal parameter set and generated 100,000 initial concentrations of the 50 proteins in the ODE model. However, the simulations' equilibrium concentrations in the "starvation" and "fed" phases, which form the initial condition for the treated phase, are uniquely determined by the nominal model's kinetic parameters and not the initial conditions, which remain identical for each simulation. From a dynamical systems perspective, stable steady states are determined by the model parameters and attract all initial conditions within their basin of attraction. As a result, a random sampling of the initial conditions has a limited impact on the model dynamics. The authors' conclusion that "the ability of expression to induce resistance also seems to be dependent on the master parameter set" can be explained by this dynamical systems perspective, where the resistance state corresponds to a stable steady state determined by the master parameter set. Considering this, the evidence presented in the manuscript may not fully support the authors' conclusion regarding the importance of protein expressions relative to protein dynamics. The discrepancy might be attributed to a possible misunderstanding of this point, and further clarification from the authors could be helpful.*

We thank the reviewer for the thoughtful perspective. We agree that, in a monostable system with fixed kinetic parameters and fixed conserved totals, varying only the initial split among moieties (e.g., X vs pX) will not change the final steady state; trajectories converge to the same attractor. In our analysis, however, “initial conditions” predominantly refer to total protein abundances (e.g., X_tot = X + pX + complexes), used as a proxy for expression heterogeneity. These totals are invariants on the simulated timescale (no synthesis/degradation in the pre-equilibration phases), and therefore alter the value of the steady state under a given parameter set. In other words, our IC sampling mostly varies conserved totals rather than merely redistributing a fixed total; hence the equilibrium reached after the starvation/fed pre-equilibrations depends on the sampled totals and the kinetics. This can be seen in the new Supplementary Figure S4, showing that changing the ICs does shift the eventual steady state even when kinetic parameters are fixed.

We have revised the text to: (1) define ICs explicitly as total abundances for multi-state species, (2) distinguish “initial split” from “conserved totals,” and (3) clarify that expression effects are context-dependent rather than universally dominant (page 4: lines 139-141 and page 10: lines 413-416)

> *(5) Additionally, it is important to note that the random sampling of 100,000 initial concentrations might not sufficiently explore the vast space of possible initial conditions. In the thought experiment mentioned earlier, where each protein can have high or low expression concentrations, there are approximately 2^(50) = ~10^(15) possible combinations of initial concentrations. Thus, the 100,000 random simulations only represent around ~1/10^(10) of the possible initial conditions in this simplistic scenario. Consequently, this limited sampling of initial conditions may not provide enough information to draw meaningful conclusions, even if the initial conditions were more directly linked to kinetic rates.*

Please see our response to Comment (3). Briefly, our ICs are continuous total abundances (conserved moieties), not binary high/low states; many IC configurations converge to the same qualitative attractors, so we estimate distributional properties rather than enumerate all combinations. Our convergence diagnostics (independent replicates and sample-size doubling) show that the meta-dynamic distributions stabilise well before N=100,000 (see Supplementary Figure S12). We have clarified this in the Supplementary Information (Error Convergence section) with the new convergence results.

> *(6) The authors implement a parameter selection step in the manuscript, where they filter out parameter sets that lead to what they term non-biological simulations. However, the rationale for determining if a given parameter set results in a stiff system of ODEs remains unclear. The authors cite references [38,39] to support the claim that stiff equations are not biologically plausible. Still, upon review, it is evident that [38] does not include the term "stiff," and [39] discusses using implicit methods to simulate stiff ODE models without specifically commenting on the biological plausibility of stiff systems. The manuscript lacks direct evidence to justify the conclusion that filtering out parameter sets that result in stiff ODE systems is reasonable. Since the filtering step accounts for the majority of discarded parameter sets, a stronger foundation is required to support the statement that stiff equations are non-biological.*

We thank the reviewer for pointing out the issue in our original justification. The reviewer is correct: stiff systems are a common feature of biological models, and our claim that they are likely 'biologically implausible' was not well substantiated. The filtering of these model instances was, in fact, due to a computational limitation rather than a biological principle. The issue was that these parameter sets produced systems of ODEs that were so numerically stiff they were unsolvable within a reasonable timeframe by the SUNDIALS ODE solver suite, which is specifically designed for such systems.

Following the reviewer's comment, we investigated the source of this prohibitive stiffness. We discovered it was not an intrinsic property of the parameter sets themselves, but rather an artifact of our simulation setup. The extreme stiffness occurred almost exclusively during the initial integration timesteps, caused by the large initial discrepancy between the concentrations of active and inactive protein forms. This large discrepancy created the conditions for overtly stiff solutions i.e. unsolvable with implemented ODE solve settings. To overcome this problem, we set a large maximum number of steps in the ODE solver for the first couple of time points, enabling the solver to overcome the excessively stiff portion of the solve. We found that the vast majority of the previously 'unsolvable' model instances could now be successfully simulated. Consequently, the number of parameter sets discarded due to solver failure is now negligible (< 1%), and this filtering step no longer accounts for the majority of discarded parameter sets. Most importantly, the distributions of dynamics were not significantly altered by this adaptation.

We have revised the " Sampling and filtering of model instances (page 5: lines 174 – 189)" part in the Methods section to reflect this more accurate understanding. We have corrected our original claim regarding the biological plausibility of stiff systems and corrected our use of the references. Ref [38] was included to demonstrate that models of biological systems are stiff, which was a major conclusion of that paper, and [39] was originally included to demonstrate that solving ODEs is reliant on solvers that can integrate stiff systems. Upon review, ref [39] has been removed.

Overall, this investigation has made our analysis more robust by allowing us to include a wider, more representative range of parameter sets, and has tangibly improved the quality of our study.

> *(7) Additionally, it is important to consider the standard method for accounting for stiff systems, as presented in [39], which involves using implicit numerical methods for ODE simulation. The authors mention using numerical methods from the SUNDIALS suite, which includes implicit methods, but the specific numerical method used remains unclear. Furthermore, it would be valuable for the authors to disclose the number of parameter sets that were filtered to obtain the final set of 100,000 accepted parameter sets. This information would provide insights into the extent of filtering and the proportion of parameter sets that were excluded during the selection process.*

We apologise for the lack of specific detail and have now updated the text. To clarify, all ODE simulations were performed using the CVODE solver from the SUNDIALS suite. This solver employs an implicit, variable-order, variable-step Backward Differentiation Formula (BDF) method, which is robust and specifically designed for handling the stiff systems common in biological network modelling. We have now explicitly stated this in the "ODE model construction, modelling, and simulations (page 4: lines 162 – 164)" section of the Methods.

Regarding the filtered parameters, we have included a revised and detailed discussion of this in the "Sampling and filtering of model instances (page 5: lines 174 – 189)" part in the Methods section (see our response to comment (6) above). Briefly, after applying the filters, ~40–45% of instances did not reach steady state within the simulation timeframe, and ~50–55% did not meet the minimum drug-response criterion. Approximately 10% satisfied all criteria and were retained for analysis. Importantly, we employed 'rejection sampling' and continued drawing until we had N = 100,000 accepted instances that satisfied all the criteria.

> *(8) An important step in the simulation process described by the authors is the simulation of the "fasted" and "fed" states until an equilibrium is reached. However, it is not clear how the authors determine if the system has reached an equilibrium. It would be helpful if the authors could provide more information regarding the criteria used to assess equilibrium in the simulations. Regarding the "fed" state, it is not explicitly stated whether the mitogen stimulus is assumed to be constant throughout the "fed" experiment. Considering the dynamic nature of mitogen stimulation in biological systems, it would be beneficial if the authors could clarify this assumption and discuss its biological relevance.*

We apologise for the lack not specifying this in the original text. A simulation was considered to have reached equilibrium when the concentration of every protein species changed by < 1% over the final 100 time steps of the simulation phase. We have now added this criterion to the "Sampling and filtering of model instances (page 5: lines 177 – 179)" part of the Methods section.

Regarding the second part of the comment, in our simulations, both the mitogenic and the drug inputs were modelled as constant, stepwise functions that, once turned on, remained at a fixed concentration for the remainder of the simulation. The biological rationale for this choice was to rigorously test for bona fide adaptive resistance. By maintaining a constant mitogenic and drug pressure, we can ensure that any observed recovery in the activity of downstream proteins is due to the internal rewiring and adaptation of the signalling network itself, rather than an artefact of the removal or decay of the external stimulus/drugs. We have now clarified this rationale in the "ODE model construction, modelling, and simulations (page 4: lines 168 – 171)" part of the Methods section.

> *(9) The "Description of Model Scope and Construction" section in the Supplementary Information should include explicitly the model reactions and some discussion about their specific form (e.g., why is '(((kc2f1*pIR*PI3K) / (1 + (pS6K/Ki2))) + (kc2f2*pFGFR*PI3K))' representing the phosphorylation rate of PI3K, with pS6K in the denominator?).*

The reviewer is right to ask for model justification. We have expanded the Supplementary "Description of Model Scope and Construction" section (page 2: line 63 – page 5: line 185) to include a complete reaction list with rate laws and a brief rationale for each. We also explain the specific PI3K phosphorylation term: activation by pIR and pFGFR is attenuated by pS6K via a denominator, which captures the well-described S6K-mediated negative feedback that reduces activation (e.g., via IRS1 phosphorylation).

> *(10) In line 349, the statement "Given that CDK46cycD is only strongly suppressed in just*

> *under 60% of the model instances (Figure 3C)" lacks clarity regarding where to look to interpret the 60% value. If this means that 4 out of the 7 model instances are resistant, and the other 2 proteins also have the same percentage of resistance, then there is no apparent reason to focus solely on CDK46cycD.*

The reviewer is correct; the figure reference was an error, which has been rectified in the main text (page 9: line 355). The actual figure reference was to Supplementary Figure 2A, which shows the heatmap of all the frequencies for each protein dynamics for all the active protein forms. CDK4/6cycD shows a sustained decreasing dynamic for 59.93% of model instances, which is where this number was derived. We have also now explicitly referenced this number in the supplementary Figure 2A legend.

We focus on CDK4/6cycD because it is the direct pharmacological target of CDK4/6 inhibitors. Our point was to suggest that even when the target is suppressed in the majority of instances (~60%), this does not reliably propagate to uniform downstream inhibition across the network, thus highlighting emergent, network-driven adaptive responses.

> *(11) We observed that in Fig. 5A, the authors show that multiple pathways are blocked. However, it is unclear whether they reduced the value of one parameter in the experiment or simulated multiple combinations of parameter inhibition. Considering the large number of parameters (94) in the model, if the authors simulated all possible combinations of parameter inhibition, the number of combinations would be significantly more than 94. An actual inhibitor typically has an inhibitory effect on multiple molecules. Therefore, it would be necessary to identify the parameters that lead to drug resistance when multiple molecules are inhibited. However, examining the inhibition patterns for all 94 parameters would be practically impossible. As a potential approach, we suggest using ensemble learning techniques, such as random forests, to handle this problem efficiently. With a dataset of binary outputs indicating the presence or absence of resistance for a sufficient number of inhibition patterns, ensemble learning can be applied to find the parameters that contribute to drug resistance. Popular feature selection algorithms like Boruta could be utilised to identify the most relevant parameters. The results obtained by ensemble learning are similar to the ranking in Fig. 5C, potentially providing a more robust validation of the authors' findings. By incorporating these additional analyses, the authors could strengthen the reliability and significance of their results related to parameter inhibition and drug resistance.*

We appreciate the suggestion and the opportunity to clarify. Figure 5A depicts multiple pathways were interrogated, but in the analysis, parameters were inhibited one at a time (OAT) - not in combination. We have revised the figure legend and added a section named “Protein knockdown perturbation analyses (page 6: lines 228 – 233)” in the Methods section to make this explicit. Moreover, some additional text in the main text has been slightly modified to make this clearer (page 11: lines 462-463, page 24: lines 856-857).

We chose the OAT design intentionally to obtain causal, first-order attribution of control points across a broad parameter ensemble without confounding from simultaneous co-inhibition. This provides an interpretable ranking of primary drivers (Figure 5C) that is consistent with the paper’s mechanistic focus. We agree that a multi-target inhibition approach could be a useful next step; however, an exhaustive combinatorial screen is beyond the scope of this proof-of-concept. In such future studies, the ensemble learning, as suggested by the reviewer, could be layered onto our MDN framework to assess robustness of the ranking under co-inhibition.

> *(12) In explaining the parameterization of the model, we find an implication of a quantitative model. However, upon examining the results in Fig. 7D, we observe that they are only qualitatively correct. When comparing Figs. 7A and 7C, we note that many model instances are immediately suppressed, and the time scale remains unknown. We*

> *believe it would be essential for the authors to explain how the model of this study maintains its quantitative nature despite the results in Fig. 7. If such an explanation cannot be provided, it raises concerns regarding the biological reliability of several findings within this study.*

While our framework is built on quantitative ODEs, the validation we present in Figure 7 is indeed qualitative. This is an intentional and key feature of our study's design. Our goal was not to build a calibrated, quantitative model of a specific cell line (e.g., MCF10A), but rather to establish a proof-of-concept theoretical framework that systematically explores the full spectrum of dynamic behaviours a given network topology can possibly generate. To achieve this, we intentionally sampled parameters from a very broad, unbiased range to delineate the theoretical upper limit of heterogeneity. This *in silico* population is therefore designed to be far more heterogeneous than any single isogenic cell line.

The striking qualitative agreement seen between our meta-dynamic distributions and the single-cell data in Figure 7D is thus not a failure of quantitative prediction, but rather a strong validation of our core premise: that a significant degree of signalling heterogeneity exists in cell populations and that our framework can effectively capture its emergent properties.

Regarding the specific comment on Figure 7C, we apologise for the lack of clarity. Nominally, we chose to simulate for 24 hours however, the x-axis in our simulations represents arbitrary time units, as the timescale is dependent on the meaning/units of the parameter values. The goal is to compare the qualitative shape of the response (e.g., rebound, sustained decrease), not the absolute time in hours. Moreover the rapid initial suppression seen in many of our model instances (Fig 7C) is a direct parallel to the rapid suppression seen in the experimental data (Fig 7A). This initial phase is followed by a wide variety of adaptive behaviours (or lack thereof) in both our simulations and the real cells, which is the key phenomenon we are studying.

We have revised the text (page 14: lines 598-601) and Figure 7's legend to state more explicitly that our validation is qualitative and to clarify the purpose of our broad, uncalibrated approach. We have also added a note in the Discussion (page 18: lines 744-747) that calibrating this framework with cell-line-specific data is a natural next step for generating quantitative, context-specific predictions.

> *(13) Related to the previous point, the experimental data is presented as fold-change during CDK4/6 inhibition, and we notice that the initial fold-change at time 0 varies between 1 and 1.8. The difference in initial fold-change is unclear to us, as our understanding of fold-change typically corresponds to the change from baseline, typically represented by the protein concentration at time 0.*
>
> *Furthermore, while the experimental data exhibits uniformly decreasing CDK4/6 activity, a substantial number of simulations indicate constant CDK4/6cycD, showing a significant qualitative discrepancy between the simulations and experimental findings. This disparity makes it difficult for us to interpret the comparison between the two datasets effectively, given the complexities in comprehending the experimental fold-change figure.*
>
> *As Figure 7 serves as the primary validation of model simulations in the manuscript, we believe that the current presentation may not provide a compelling reason to believe that the model accurately captures experimental data. To enhance clarity and validation, we suggest overlaying the experimental data over the simulations or considering the median and 10/90% percentile of the experimental data, which may potentially offer improved readability and facilitate a more robust interpretation of the comparison.*

The experimental data from Yang et al. (ref 55, main text) measures kinase activity using a

nucleus-to-cytoplasm translocation reporter system, wherein a bait protein is phosphorylated by the target kinase causing it to translocate from the nucleus to the cytoplasm. Hence, the y-axis represents the ratio of nuclear vs. cytoplasmic fluorescence, not a fold-change from a t=0 baseline. The variation in the starting value (between 1 and 1.8) reflects the inherent heterogeneity in the reporter's localization across individual cells even before the drug is added. We have updated the y-axis label and revised Fig. 7's legend to state this explicitly.

The most likely explanation for the discrepancy between experimental dynamics and our simulation dynamics is that the experimental data comes from an isogenic cell line that is largely sensitive to CDK4/6 inhibition. Our simulations are derived from a very wide parameter sweep, where the intent is to represent all possible cell states. It is quite striking that that there is such a high correlation between the experimental data and simulations, indicating that perhaps the heterogeneity of even isogenic cell lines is significantly greater than might be intuited; a point we now mention in the revised Discussion (page 17: lines 716-727).

It is worth noting again, that our analysis is intentionally constructed to be as heterogeneous as possible, and is not trained on any biological data that might otherwise constrain the output-behaviour space. The isogenic cell line almost certainly represents a much more constrained output-behaviour space than our analysis.

The y-axis label has also been updated accordingly. As mentioned in (12) this result is intended as a qualitative validation, showing that cell lines indeed have highly variable signalling dynamics. Given the range of parameters tested, we think it is surprising that the degree of agreement between the experiment and our analysis is as high as it is. Again, we believe this suggests that heterogeneity may be more prevalent than is intuited. We do not believe we have made any strong quantitative claims in the main text, and we certainly aim to work towards biological, quantitative validation in the future. Finally, we altered the wording of the results heading (page 14: line 562) to make it clear that we are only making qualitative claims and removed the claim that the evidence was strong.

With these clarifications and corrections, we believe the validation is now much more compelling. The key point is not a perfect quantitative match, but the strong similarity in the distribution of heterogeneous behaviours.

> *(14) The authors mention simulating treatment with 10nM of CDK4/6i or Ei, but specific details on how this treatment is included in the model simulations are not provided. This lack of information makes it challenging to fully evaluate the comparison between model simulations and experimental evidence in Figure 7. It would be highly appreciated if the authors could clarify how the treatment with CDK4/6i or Ei is incorporated into the simulations to facilitate a better understanding and interpretation of the results.*

To clarify, the effects of the inhibitors were incorporated directly into the kinetic rate laws of their respective target reactions.

CDK4/6 inhibitor (CDK4/6i): This was modelled as an inhibitor of the formation of the active CDK4/6-cyclin D complex. We have now explicitly detailed this in the description for reaction R27 in the "Description of Model Scope and Construction" section of the Supplementary Information.

Estrogen Receptor inhibitor (Ei): This was modelled as an inhibitor of the estrogen-dependent activation of the Estrogen Receptor. This is now explicitly detailed in the description for reaction R15 in the same supplementary section.

It is however important to reiterate that our goal in Figure 7 is qualitative, shape-based comparison; therefore, we used a fixed fractional inhibition (reported in Methods) rather than a calibrated IC50/Hill model.

> *(15) The authors state strong support for their modelling conclusions based on the literature. However, we still have concerns regarding the validation of the model against CDK2 or CDK4/6 data in Figure 7, as it appears less convincing to us. Furthermore, the authors list known resistance mechanisms that are replicated in their modelling. Nevertheless, we find the conclusion somewhat weakened by Figure S10, where approximately 80% of the nodes are implicated in some form of resistance pathway. This raises questions about the model's selectivity, as many proteins included in the model seem to drive resistance in some manner. In the Supplementary Information, the authors mention excluding or abstracting some protein species from the mitogenic and cell cycle pathways to manage computational resources effectively. This abstraction makes it difficult to determine if the proteins identified as potential drivers of resistance genuinely drive resistance or might represent abstractions of other potential drivers. To enhance the manuscript's clarity and address potential concerns about the model's selectivity and abstraction, we suggest providing more details and discussion in the main text.*

The reviewer's observation that a large number of nodes are implicated in resistance pathways in Figure S10 is correct. However, we argue this is not a weakness of the model's selectivity, but rather a key finding that reflects the biological reality of adaptive resistance. The literature is replete with a wide and growing number of distinct mechanisms of resistance even to a single class of drugs (1,2), which supports the idea that cancer can co-opt a wide variety of network nodes to survive.

Figure S10 is not a binary map where every implicated node is equal, instead it is a likelihood map, where the colour and weight of the connections represent how often a particular interaction participates in driving resistance across the theoretical full range of possible network dynamics. The figure shows that while many nodes can contribute to resistance, they do so in a hub-like manner i.e. small subsets of nodes coordinate to drive resistance. This provides a rationalised, data-driven prioritisation of the most dominant and recurrent resistance strategies. We draw two important conclusions from this work 1) Resistance likely occurs due to resistance hubs, not individual proteins, and 2) that the frequency of a resistance hub in an MDN analysis is likely proportional to the frequency of that hub emerging as a resistance mechanism in a population of cells and patients.

Regarding the issue of abstraction, the reviewer is correct that this is an inherent feature of any tractable systems model. In our case, several species in the mitogenic/cell-cycle pathways are module-level proxies to control model size. The highly implicated "hub" nodes in our model likely represent critical cellular processes that are themselves composed of several individual protein interactions.

To address these concerns, we have significantly revised the Discussion (page 16: lines 681 – 694) to: (1) frame resistance as a network-level phenomenon; (2) show that our frequency-based ranking is selective, prioritising the most probable, recurrent mechanisms; and (3) clarify that - given model abstraction -our findings implicate critical processes (modules), not just single proteins, as the drivers.

Overall, these changes do not alter our main conclusions: adaptive resistance is an emergent, network-level property; many routes exist, but a smaller set of nodes/modules consistently carry the largest influence across heterogeneous contexts.

> *(16) We consider that the figures and legends, including the supplementary information, are inadequately explained. The information provided is insufficient for us to comprehend the figures fully, leading to the need for interpretation on our part as readers. This could potentially introduce biases when trying to understand the claims made by the authors. To improve our understanding, it would be essential for the authors to assign appropriate labels to the figures and provide comprehensive*

> *explanations in the legends. For example, in Fig 3, we suggest labelling the tree diagrams in panels A and B, as well as the colour bars. We also recommend applying the same approach to other figures, adding accurate axis labels and descriptions of colour gradients to enhance clarity.*

We thank the reviewer for this critical feedback. To address this comment, the figure legends have been revised where appropriate and greatly expanded to improve their comprehension. Moreover, we have added explicit labels to all previously unlabelled components, such as the cluster dendrograms and colour code bars in Figure 3A, B.

> *(17) To enhance readability, we recommend interchanging the order of Figures 1 and 2 in the sequence they appear in the main text. Alternatively, the text can be adjusted to refer to the figures in the correct order. Additionally, attention should be given to the bottom of Fig 1, which appears to be cropped or cut off. Furthermore, the incorrect word spacing in some figure elements, such as Fig. 3A title, Fig. 5B title, and Fig. 6B y-label, should be corrected for improved visual presentation.*

Following the reviewer's comment, the order of Figures 1 and 2 has been switched to reflect the order in which they are referred to in the main text. These Figures have been re-exported to fix unintentional word spacing errors.

> *(18) We recommend that the language used to refer to the initial conditions in the manuscript is clarified and homogenised. Currently, the authors use different terms such as "basal expression," "protein expression," "state variable values," or "initial conditions" to refer to them. This variation in terminology can be confusing for readers. In particular, the use of "basal expression" is problematic, as it typically refers to the leaky value of a reaction in the absence of an inducer, making it another biophysical parameter of the system rather than an initial condition. To enhance clarity and consistency, we suggest the authors decide on a single term to refer to the initial conditions throughout the manuscript and provide a clear explanation of its meaning to avoid any confusion. This will help readers better understand the concept being discussed and prevent any potential misinterpretations.*

We thank the reviewer for this very helpful suggestion. To resolve this and improve clarity, we have homogenized the language throughout the manuscript. We now clarify the use the following 3 terms in their specific contexts:

We use "protein abundances" exclusively for the conserved total abundances of multi-state species (e.g., Xtot = X + pX + complexes) that are sampled across instances to represent expression heterogeneity.

We use 'initial conditions' to refer to initial values of the state variables in a model simulation. This term is related to protein abundance as the setting of initial conditions for conserved species sets the protein abundance. This is explicitly stated in the text (page 3: lines 87 - 91).

We use "state variables" to refer to the time-dependent model species.

We avoid the term "basal expression" in technical descriptions. Where a biology-facing phrase is helpful, we use "protein expression level". This is used when referring to the biological concept that the initial conditions are intended to represent, i.e. the heterogeneity in protein amounts across a cell population.

We have performed a thorough search-and-replace to ensure this new convention is applied consistently and have removed the potentially confusing term "basal expression" from the revised manuscript.

> *(19) Why are saturable functions (e.g., Michaelis-Menten functions) ignored in the model? What are the potential consequences?*

The main objective of this work was to perform a large-scale, systematic exploration of a high-dimensional parameter space (94 parameters) to map the full repertoire of qualitative dynamic behaviours a network topology can support. Using saturable functions like Michaelis-Menten kinetics would have roughly doubled the number of parameters to be explored (from k to Vmax and Km for each enzymatic reaction), making a parameter sweep of this scale computationally intractable. We therefore prioritised the breadth of the parameter search over the depth of kinetic detail, which we believe is the appropriate choice for a proof-of-concept study focused on heterogeneity.

This simplification has potential consequences. A major one is that our model cannot capture phenomena that arise specifically from enzyme saturation, such as zero-order kinetics or certain forms of ultrasensitivity (switch-like responses). However, we argue that this is an acceptable trade-off for two main reasons: (1) Our analysis is based on classifying broad, qualitative response shapes (increasing, decreasing, rebound, etc.). Mass-action kinetics are fully capable of generating this rich spectrum of behaviours; and (2) by varying the mass-action rate constants over nine orders of magnitude (from 10^{-5} to 10), our parameter sweep effectively samples a vast range of reaction efficiencies. A very low rate-constant can approximate the behaviour of a saturated, low-efficiency enzyme, while a high rate-constant can approximate a highly efficient, non-saturated one. In this way, the broad sweep of the rate parameter partially reflects the effects that would be captured by varying Vmax and Km.

For transparency, we have added a brief rationale to the “ODE model construction, modelling, and simulations” part of the Methods (revised main text, page 4: lines 153-155) and the "Description of Model Scope and Construction" section in the Supplementary file (Supplementary text page 2: lines 63-73).

> *(20) Given the relevance of the concept of "heterogeneity" in this work, a short discussion about biochemical noise and its implications on the analysis (e.g., why it is not included, and if it will be a next step) would be appreciated.*

Our MDN modelling framework represents heterogeneity by creating an ensemble of deterministic models, where each model instance has a unique set of kinetic parameters and/or initial protein abundances. We propose that this is a powerful way to mechanistically represent the functional consequences of all sources of cellular variation. Over time, the effects of genetic mutations, epigenetic states, and even the time-averaged impact of intrinsic biochemical noise will manifest as changes in the effective interaction strengths and protein concentrations within a cell. Our large-scale parameter/IC sweep is designed to systematically explore the full range of dynamic behaviours that can emerge from this underlying biological variation. Therefore, our approach does not compete with stochastic modelling but is complementary to it. While stochastic simulations can capture the dynamic trajectories of single cells, our framework provides a panoramic view of the entire spectrum of possible stable phenotypes that can emerge at the population level. We agree that modelling intrinsic biochemical noise (stochasticity arising from finite copy numbers), e.g. using chemical Langevin or SSA, is a possible extension in future work but expected to be very computationally expensive. We have added a brief discussion on this as future direction in the revised Discussion.

> *(21) We have noticed that the first four paragraphs of the Discussion section overlap with the Introduction, as they mainly reiterate the significance of the study itself rather than focusing on the specific results obtained. To avoid redundancy and provide a more cohesive and informative discussion, we recommend that the authors shift the focus of the Discussion section towards presenting potential interpretations, even if they are not*

> *definitive, of the results obtained. By doing so, the Discussion will serve as a valuable platform for deeper analysis and insightful observations, allowing readers to better comprehend the implications and significance of the research findings.*

We thank the reviewer for this structural feedback. Following the reviewer's feedback, we have significantly rewritten and restructured the Discussion section. The redundant introductory material has been removed.

The rewritten Discussion centres on interpretation, implications, and connect our findings to the literature. It now: (i) frames MDN as a systems-level framework that links molecular heterogeneity to qualitative signalling “meta-dynamics” and adaptive escape under constant drug pressure; (ii) highlights two key findings: an asymmetry in control (interaction kinetics exert stronger, more consistent influence than protein abundance) and a topology-driven convergence whereby a vast parameter space funnels into a finite set of recurrent behaviours; (iii) shows that resistance is a network-level property, with many possible routes but a small set of recurrent hubs/modules dominating; and (iv) provides a qualitative alignment with single-cell reporter data while clarifying the intent and limits of that comparison. Moreover, we now explicitly discuss limitations (rate-law simplifications, broad priors, determinism, and modular abstractions) and outline next steps for future research, including data-constrained priors and stochastic extensions.

We believe this substantial revision has transformed the Discussion into a much more insightful and valuable part of the manuscript that directly addresses the reviewer's concerns.

> *(22) The supplemental text file containing the model equations can be a bit challenging to read and understand. It would be greatly beneficial if the authors could consider generating a file using a typesetting program.*

We have now included a typeset list of state variable equations and ODEs, along with the original model files.

> *(23) The authors mentioned that some model parameterizations result in negative solutions, which is surprising. Access to the model equations would help understand why this happens and is crucial for researchers who may want to use this approach. Clarifying the model equations' presentation would enhance transparency and aid other researchers in applying this method for similar research questions.ach. Clarifying the model equations' presentation would enhance transparency and aid other researchers in applying this method for similar research questions.*

The reviewer is correct to be surprised by the mention of negative solutions, as negative concentrations are physically impossible. We clarify that these are not a result of any structural flaw in our model's equations but are a well-known, although rare, numerical artifact of floating-point arithmetic in computational solvers.

Our model is constructed using standard mass-action and first-order kinetics, which structurally guarantee non-negativity. However, when a species' concentration approaches the limits of machine precision (i.e., becomes a very small number extremely close to zero), the ODE solver can, in rare instances, numerically undershoot zero, resulting in a small negative value. If this occurs, it can lead to instability in subsequent integration steps.

This is not a biological phenomenon but a computational one. Therefore, the standard and appropriate procedure, which we follow, is to implement a filter that discards any simulation trajectory where such a numerical instability occurs.

> *(24) The reference listed for the CDK4/6 and CDK2 measurements is Yang et al. [55] in the figure caption, but as Xe et al. in lines 559-561 of the manuscript.*

The text has been updated to match citation.

> *(25) We suggest that the authors revise and cite a previous study conducted by Yamada et al. (Scientific Reports, 2018), which presents an approach to expressing cell heterogeneity as a probability distribution of model parameters.*

Following this suggestion, we have revised the Discussion (see response to comment (21)) to include and discuss Yamada et al. (Scientific Reports, 2018), which models cell heterogeneity as a probability distribution over parameter values.

> *(26) In the manuscript, on line 677, the authors state, "This indicates that there is an upper limit to the degree to which parameter sets can influence the qualitative shape of a protein's dynamic within a given network topology." We wish to highlight that this finding may not be particularly surprising. Given that the parameters were randomly determined within a specific range, it is understandable that altering the number of parameter samples would not substantially impact the distribution of model instances.*

We thank the reviewer for this insightful comment, which allows us to clarify the significance of this finding. While it is true that any sampling from a fixed distribution will eventually converge statistically, our conclusion is not about statistics but about the intrinsic, constraining properties of the network's topology. The novelty is not that the distribution converges, but that it converges to a surprisingly limited and finite repertoire of qualitative dynamic behaviours. A complex, non-linear network with nearly 100 free parameters could theoretically generate an almost endless variety of complex dynamics. Our finding is that this specific biological topology acts as a powerful filter, robustly channelling the vast majority of the near-infinite parameter combinations into a small, recurring set of functional outputs (increasing, decreasing, rebound, etc.).

The reason for this finite limit is mechanistic, as the reviewer's comment prompted us to investigate further. Our parameter sweep already covers an extremely wide, 9-order-of-magnitude range. As we pushed parameter values to even greater extremes in exploratory simulations, we found they do not generate novel, complex dynamic shapes. Instead, they tend to drive network nodes into saturated states- either permanently "on" (maximally activated) or permanently "off" (minimally activated). In both cases, the node becomes unresponsive to upstream perturbations.

Therefore, further expanding the parameter range would be unlikely to uncover new behavioural categories; it would simply increase the proportion of model instances classified as "no-response." This demonstrates a fundamental principle: the network topology itself enforces an upper limit on its dynamic complexity. We think this inherent robustness is what allows for reliable cellular signalling in the face of constant biological variation. We believe this is a non-trivial finding, and we have revised the Discussion (page 16: lines 664 - 680) to state this conclusion and its implications more clearly.

https://doi.org/10.7554/eLife.87710.2.sa0